Urea Recovery from Human Urine Using Nanofiltration and Reverse Osmosis

by

Lucas Crane

A Thesis Presented in Partial Fulfillment
of the Requirements for the Degree
Master of Science

Approved April 2022 by the
Graduate Supervisory Committee:

Treavor H. Boyer, Chair
Francois Perreault
Paul Westerhoff

ARIZONA STATE UNIVERSITY

May 2022

ABSTRACT

Global shortages of urea and unsustainable production of synthetic urea have caused concerns over the future of food production, automobile operation, and other processes. Urine is a waste product that could supplement synthetic urea production. This study utilizes polyamide reverse osmosis (RO) and nanofiltration (NF) membranes in a cross-flow orientation to selectively recover urea from fresh human urine. Urea permeation experiments were conducted to determine the effects of urea stabilization via pH adjustment and membrane type on the production of a pure urea product. Fouling mitigation experiments were then conducted to determine the efficacy of microfiltration (MF) pretreatment on the reduction of the membrane fouling layer. The results showed that the NF90 membrane had advantageous performance to the BW30 RO and NF270 membranes, permeating 76% of the urea while rejecting 68% of the conductivity. Urine stabilization via acetic acid or sodium hydroxide addition did not inhibit membrane performance, signifying the use of pH 5 as a suitable pretreatment condition. Real fresh urine had higher rejection of constituents for NF90, suggesting the reduction of the membrane's effective pore size by organic material. MF pretreatment reduced foulant thickness and permeate flux loss but did not change the speciation of microorganisms. Finally, different urea-based products, such as fertilizers, biocement, and synthetic polymers, were suggested to show the potential of urine-recovered urea to reduce costs. The results from this work show the efficacy of using polyamide RO and NF membranes to supplement unsustainable synthetic production of urea with sustainably sourced urea from a waste product, human urine.

DEDICATION

To my family, friends, and girlfriend for their love, insight, and constant support of me and my goals. Thank you for being a part of my life.

ACKNOWLEDGEMENTS

I would like to thank Dr. Treavor Boyer, who approached me years ago to conduct research with him. Since then, I have had the opportunity to work on exciting topics that I truly believe have impact, and I could not ask for more in a mentor. Thank you for continuously challenging me and helping me think in new and improved ways.

I would like to thank my committee members, Dr. Francois Perreault and Dr. Paul Westerhoff, for their guidance on my research and for setting out the time for this project. Your insight on this project has helped propel this research forward and, in the process, has helped me approach this research in new ways.

This work was supported by the Science and Technologies for Phosphorus Sustainability (STEPS) Center, a National Science Foundation Science and Technology Center (CBET-2019435). Any opinions, findings, and conclusions or recommendations expressed in this material are those of the authors and do not necessarily reflect those of the NSF.

TABLE OF CONTENTS

Page

LIST OF TABLES v

LIST OF FIGURES vi

CHAPTER

1 INTRODUCTION 1

2 MATERIALS AND METHODS 8

Fresh Human Urine 8

RO/NF Membranes 9

RO/NF System 9

RO/NF Urea Permeation Experiments 10

RO/NF Fouling Experiments 12

Cleaning 13

Economic Analysis 14

Analytical Methods 14

Data Analysis 15

3 RESULTS AND DISCUSSION 17

Evaluation of pH Pretreatment Conditions and Membrane Types for SFU 17

Comparison of RFU With SFU for Best pH Condition 24

Fouling Mitigation With MF Pretreatment 26

Economic Analysis Of Different Urea-Based Product 33

4 CONCLUSION 36

REFERENCES 38

APPENDIX Page

A SUPPLEMENTARY FIGURES 45

B SUPPLEMENTARY TABLES.. 56

LIST OF TABLES

Table Page

1. Different Commercially Available Urea-Based Products 34

LIST OF FIGURES

Figure Page

1. Conceptual Diagram of Process. 7

2. Urea Permeation Results for SFU Experiments, Across Three Ph Pretreatment Conditions and Three Membranes. 19

3. Conductivity Rejection Results for SFU Experiments, Across Three pH Pretreatment Conditions and Three Membranes. 21

4. Specific Ion Rejection Results for SFU Experiments, Across Three Ph Pretreatment Conditions and Two Membranes: (a) BW30 RO, (b) NF90, And (c) NF270. 23

5. Rejection of Different Compounds by BW30 RO, NF90, and NF270, From RFU. 25

6. Comparison of SFU and RFU Experiments for (a) Urea Permeation And (b) Conductivity Rejection. 26

7. Permeate Flow Reduction Over the 24 h Period for Experiments With and Without MF Pretreatment. 27

8. Fouled Membranes After 24 h Experiments, With (a) No MF Pretreatment and (b) MF Pretreatment. 28

9. FTIR Analysis Results for Two Treatment Conditions, With Duplicates, Compared to Virgin NF90 Membrane. 29

10. SEM Imagery of Virgin NF90 Membrane, at (a) 100-Times Magnification and (b) 28,000-Times Magnification. 30

Figure Page

11. SEM Imagery of Biofouled NF90 Membrane for Experiments With No MF Pretreatment, for Duplicate 1 at (a) 500-Times Magnification and (b) 5,000-Times Magnification; and for Duplicate 2 at (c) 2,000-Times Magnification and (d) 1,000-Times Magnification. 31

12. SEM Imagery of Biofouled NF90 Membranes for Experiments With MF Pretreatment, for Duplicate 1 at (a) 500-Times Magnification, (b) 1,000-Times Magnification, and (c) 5,000-Times Magnification; for Duplicate 2 at (d) 5,000-Times Magnification. 32

CHAPTER 1

INTRODUCTION

Urea is a high value chemical used most commonly for fertilizers but also for novel materials such as diesel exhaust fluid, biocement, polymeric adhesives, and elastomers. However, natural gas price increases and geopolitical instability have caused global urea shortages and increases in urea prices that threaten global food markets and the production of other products that rely on urea (King, 2021; Quinn, 2022; Zhong, 2021). Furthermore, urea used for these processes is synthetically produced through the conversion of nitrogen gas into ammonia (NH_3) via the Haber-Bosch process and the combination of NH_3 with carbon dioxide (CO_2) under high temperatures and pressures to produce urea (Boerner, 2019; Patel, 2020); the production of synthetic urea is thus energy intensive and produces greenhouse gas emissions. Given these global shortages and unsustainable production, new sustainable sources of urea are needed.

Urine is a waste product that is produced at a rate of approximately 11 g/cap/day N (Rose et al., 2015). Given its wide availability and high concentration of urea, urine could be used to supplement global urea shortages. The collection of urine for urea recovery would require diversion of urine away from centralized wastewater treatment systems; doing so would reduce the nutrient loads on wastewater treatment plants and increase operating efficiency, as literature has shown that urine contributes to 80% of the total nitrogen (TN) and 50% of the total phosphorus (TP) but only 1% of the total volumetric flow of wastewater (J. Wilsenach & van Loosdrecht, 2003). Different urine treatment processes have been studied to recover nitrogen, including precipitation of struvite (Antonini et al., 2011; Hug & Udert, 2013; N. Jagtap & Boyer, 2018; Lind et al., 2000;

Ronteltap et al., 2007a, 2007b, 2010; J. A. Wilsenach et al., 2007; Xu et al., 2017), air stripping of NH_3 gas (Antonini et al., 2011; Başakçilardan-Kabakci et al., 2007; N. Jagtap & Boyer, 2018; B. Liu et al., 2015; Xu et al., 2017), biological nitrification of NH_3 in urine (Christiaens et al., 2019; Feng et al., 2008; Udert, Fux, et al., 2003), and adsorption of ammonium (NH_4^+) onto ion exchange resins (Ganrot et al., 2007; Pradhan et al., 2017; Tarpeh et al., 2017). A common theme in most literature on nitrogen recovery from urine is the assumption that the urea hydrolysis pathway has gone to completion, i.e.,

$$(NH_2)_2CO + H_2O \xrightarrow{\text{urease}} CO_2 + 2NH_3 \qquad (1)$$

where in the presence of the urease enzyme, urea will rapidly hydrolyze into NH_3 and CO_2 (Kistiakowsky & Rosenberg, 1952; Ray et al., 2018). In order to recover urea from urine, inhibition of the urea hydrolysis pathway is necessary. Previous research has shown that pH adjustment of urine to below pH 5 (e.g., using acetic acid) or above pH 12 (e.g., using sodium hydroxide, calcium hydroxide, or magnesium hydroxide) can inhibit the urease enzyme and thus prevent the enzymatic hydrolysis of urea into NH_3/NH_4^+, allowing for the recovery of urea (Randall et al., 2016; Ray et al., 2018; Vasiljev et al., 2022). This process has been described as urea or urine stabilization, where the urea hydrolysis process has been inhibited and the collected urine maintains the nitrogen speciation (i.e., in the urea form) as when it immediately came out of the human body. Thus, this collected urine has been referred to as "fresh" human urine, while collected urine that has not been stabilized and has nitrogen in the NH_3/NH_4^+ form has been referred to as "hydrolyzed," "stored," or "aged" human urine.

Given the prevention of the urea hydrolysis reaction, membranes are a suitable technology for urea recovery from fresh human urine. Rejection of a constituent via a membrane can be modeled by the following equation:

$$R = \left(1 - \frac{C_p}{C_f}\right) * 100 \tag{2}$$

where C_p is the permeate concentration and C_f is the feed concentration. Membrane rejection occurs via two mechanisms: (1) electrostatic (Donnan) rejection, whereby charged molecules are rejected because of the negative surface charge of membranes (Childress & Elimelech, 1996; Donnan, 1995), and size (steric) exclusion, whereby molecules larger than the pore size of the membranes can not permeate through and thus are rejected (Bowen et al., 1997; Szymczyk & Fievet, 2005). Urea is a unique molecule in that it is neutrally charged, so it is not affected by electrostatic forces from the membrane surface, and is relatively small, so it is not excluded by membranes with large enough pore sizes (Courtney & Randall, 2022; Ray et al., 2019, 2020). However, other constituents in urine, such as ions, organic materials, and pharmaceuticals, are charged and/or are large compounds that are rejected at high rates (Courtney & Randall, 2022; Pronk et al., 2006; Ray et al., 2019, 2020, 2022). Literature has shown that polyamide brackish-water (BW) reverse osmosis (RO) (i.e., BW30 RO) or nanofiltration (NF) membranes (i.e., NF90) allow for permeation of urea through membranes while rejecting other urine constituents (Ray et al., 2020). However, previous literature on urea recovery from urine utilized membrane filtration in a dead-end orientation (i.e., where flow runs perpendicular to the membrane surface, resulting in formation of a “cake” fouling layer). Operation of membrane treatment systems in a dead-end orientation can cause operational problems due to increasing thickness of the cake layer, resulting in lowered flux through the membrane; operation of membrane treatment systems in a cross-flow orientation (i.e., where flow runs parallel to the membrane surface, resulting in formation of a “gel” fouling layer) allows for reduction of flux loss due to resuspension of particles in the foulant by the parallel flow (Murkes & Carlsson, 1988). This in turn allows for longer lifetimes of membranes and lowered frequency of membrane cleaning. According to the author’s knowledge, no studies have been published that have evaluated the recovery of urea in the permeate using polyamide BWRO and NF membranes in a cross-flow orientation.

Importantly, commercial manufacturers of membranes specify pH operating conditions under which membranes can guarantee performance. For membranes such as BW30 RO and NF90, these pH operating conditions range between pH 2 and pH 11. Given the need to prevent urea hydrolysis during membrane treatment of urine for urea recovery, use of a high pH condition such as pH 12 could have negative effects on performance; previous literature showed that NF90 membranes in a dead-end orientation had lowered performance at pH 12.5 due to expansion of membrane pores (Ray et al., 2020). Previous literature also showed that membrane treatment of stabilized urine using a polyamide seawater RO membrane had higher rejection of urine constituents for acid-stabilized urine than base-stabilized urine (Courtney & Randall, 2022). However, according to the author’s knowledge, no studies have been published that have evaluated the effects of urea stabilization on membrane performance using polyamide BWRO and NF membranes in a cross-flow orientation. Additionally, while previous studies specifically used BW30 RO and NF90 membranes for urea recovery from urine, literature suggests that NF270 could be a suitable polyamide membrane for recovery of urea, as NF270 has been shown to have low rejection of neutrally-charged organic compounds (Breitner, 2017) but can reject multivalent compounds (Donnan, 1995; Li et al., 2018; Wu et al., 2016). Commercial specifications suggest a high salt rejection (measured using magnesium sulfate) for spiral-wound elements (*Dow Filmtec Membranes | Flat Sheet Membrane Chart*, n.d.). According to the author's knowledge, no published studies have been published that evaluated urea recovery from human urine using NF270 membranes.

In order to ensure long-term performance of membrane systems, fouling of membranes must be considered and mitigated. Due to microorganisms commonly found on bathroom surfaces and high concentrations of ions in human urine, membrane systems can build up a fouling layer on the active side of their membranes that consist of organic constituents in urine, microorganisms, and inorganic precipitate (Ray et al., 2022). Urine stabilization via acetic acid has been shown to alter the microbiome of fresh urine during storage (Saetta et al., 2020). However, according to the author's knowledge, no previous studies have been published that evaluated the effects of urine stabilization on the fouling layer buildup during cross-flow operation of a membrane treatment system. Furthermore, previous studies have shown that pretreatment of urine using microfiltration (MF) successfully reduced the foulant thickness during cross-flow RO/NF treatment of hydrolyzed human urine, as many biological constituents in hydrolyzed human urine are larger than the pore size of microfilters (Ray et al., 2022). However, according to the author's knowledge, no studies have been published that evaluated the mitigation of MF pretreatment on fresh human urine, which contains a different microbiome than that of hydrolyzed human urine.

Thus, the goal of this research is to evaluate the recovery of urea from fresh human urine and mitigate fouling using cross-flow RO/NF membranes. A conceptual diagram of different considerations for the process can be seen in Figure 1. Three pH pretreatment conditions were evaluated to determine the effects of urea stabilization via acid or base addition on membrane performance. Three polyamide membranes were evaluated to determine the effects of membrane type and pore size on permeation of urea and rejection of other constituents. Finally, MF pretreatment of fresh human urine was evaluated to determine the potential of MF to mitigate fouling of membranes. The specific objectives of this research were to: (1) investigate the role of pH adjustment in the recovery of urea using synthetic fresh urine (SFU), (2) investigate the role of different commercial RO/NF membranes in the recovery of urea using SFU, (3) demonstrate the efficacy of the RO/NF system for the recovery of urea using real fresh urine (RFU) pretreated with MF, (4) investigate how MF pretreatment of RFU affects the fouling behavior of RO/NF membranes, and (5) suggest different urea-based products that urine-recovered urea could make more inexpensive and feasible to produce.

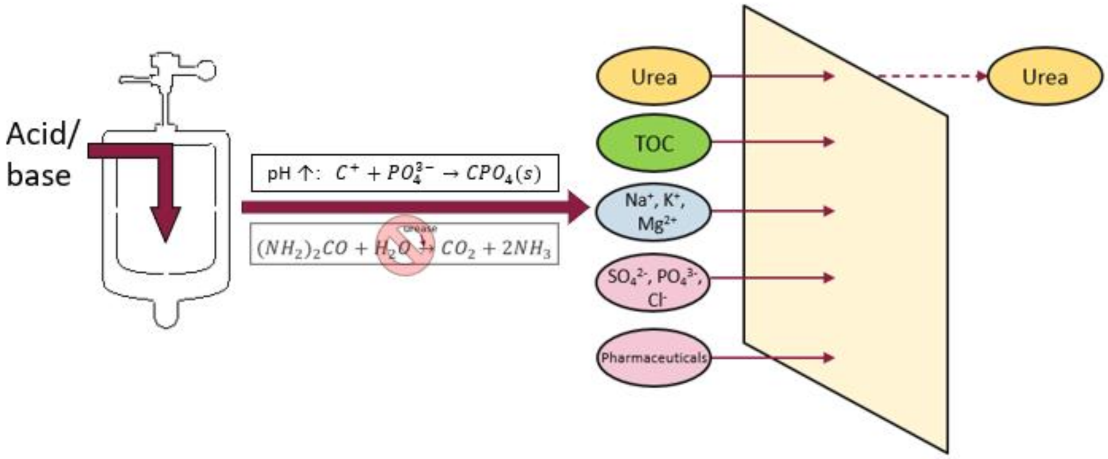

Figure 1. Conceptual diagram of process.

CHAPTER 2

MATERIALS AND METHODS

2.1. Fresh human urine

Synthetic and real fresh urine were each used in this study. Preparation of SFU was based on previous literature (Ray et al., 2019), as seen in Table S1. Sodium hydroxide (10 M) was added to SFU to adjust its pH to 6 immediately prior to use (approximately 3.8 mL), mimicking the approximate pH of real-fresh urine. After pH adjustment to 6, adjustment to pH 5 or pH 12 was done with concentrated (17.4 M) acetic acid (approximately 3 mL) or 10 M sodium hydroxide (approximately 51 mL), respectively.

Real fresh urine was collected using a portable urinal setup designed for urine collection and study. A Sloan Water-Free urinal and 17-gal storage tank were mounted on a metal frame, and the storage tank had pH, conductivity, and temperature sensors (Atlas Scientific) measuring every five minutes. Additional details on the portable urinal setup can be found in previous literature (Saetta et al., 2020). Pictures of the portable urinal setup can be found in Figures S1 through S3. The portable urinal was placed inside a men’s restroom located in a research building at the Arizona State University (ASU) Tempe campus. Acetic acid (2.5 eq/L) was pumped into the waterless urinal to ensure that the urine was maintained below pH 5 during storage; 2.5 mL of 2.5 eq/L acetic acid was added every hour overnight, from 5:00 pm–8:00 am, based on knowledge gained from previous literature (Saetta et al., 2020). The age range of urine donors was from 18–50. Only males were included in the study. Collection of human urine was approved by the ASU Institutional Review Board.

2.2. RO/NF Membranes

Three commercial membranes were used in this study: a loose RO membrane, BW30 (Filmtec); a tight NF membrane, NF90 (Filmtec); and a loose NF membrane, NF270 (Filmtec). The commercial specifications of these membranes, including salt rejection, flux, operating pH range, and material type, can be found in Table S2 (*Dow Filmtec Membranes | Flat Sheet Membrane Chart*, n.d.).

Membranes were prepped before experiment. Each membrane was cut to fit within the membrane cell without leaking, and cut membranes were soaked in a 50% isopropanol/50% ultrapure water solution for at least 20 minutes. Membranes were then transferred to deionized (DI) water to soak for at least ten minutes. The DI water was drained, and the membranes were soaked in fresh distilled water for at least ten minutes. The active area of the membranes within the system was 8.4 cm by 4.6 cm.

2.3. RO/NF System

The membrane system used in this study was that used in previous literature (Ray et al., 2022). Pictures of the system and different components can be seen in Figures S4 through S7. The membrane system consisted of a 5-gal tank that fed into a stainless-steel Swagelok membrane treatment system, fitted with a pressure gauge and needle valve for controlling the pressure of the system. To ensure a constant urine temperature, a 3/8”-diameter, 50’ stainless-steel wort chiller, made by NY Brew Supply, was placed within the 5-gal feed tank and was connected to the building’s process cooling water supply. The

Swagelok membrane treatment system was connected to a 5”-by-3/8”-by-2.5” stainless-steel membrane cell, which was made by the ASU machine shop, as well as two flow meters: a feed flow meter (Cole-Parmer, F-40375LN-6) and a permeate flow meter (Sensirion, SLI-2000). Urine and other solutions running through the system were circulated back into the feed tank.

2.4. RO/NF Urea Permeation Experiments

Urea permeation experiments were conducted to determine the effect of different pH pretreatment conditions and different commercial membranes on the permeation of urea and rejection of other urine constituents. Ten liters (2.6 gal) of SFU were added to the 5-gal feed tank, and the system was run at an operating pressure of 375 psi, a feed velocity of 37.8 cm/s (i.e., a volumetric flow rate of 1 LPM), and a temperature of 20 °C, as conducted in previous literature (Ray et al., 2022). A wetted membrane was loaded into the membrane cell, and a spacer was placed between the feed flow and the active side of the membrane to mimic conditions of a real-world spiral-wound membrane system. Waterproof plumber’s grease was used to seal the membrane cell to reduce leaking and ensure that the collected permeate was not contaminated by feed solution surpassing the membrane. A sample of the urine was taken before the experiment, and a t = 0 sample was taken after running the system for 10 min to ensure that any DI water in the system leftover from cleaning was fully mixed into the urine. The system was run until at least 20 mL of permeate was collected, and the pH and conductivity of the undiluted urine, t = 0, and permeate samples were measured. Samples were stored at 4 °C, and total nitrogen (TN) and total organic carbon (TOC) were measured on unfiltered samples. Samples were then filtered through nylon syringe filters with a pore size of 0.45 µm, and total ammonium nitrogen (TAN), chloride (Cl^-), sulfate (SO_4^{2-}), phosphate (PO_4^{3-}), sodium (Na^+), potassium (K^+), calcium (Ca^{2+}), and magnesium (Mg^{2+}) were measured. Total ammonium nitrogen represented the addition of unionized ammonia (NH_3) and ionized ammonium (NH_4^+). Each condition was run in duplicate, and the experiment was repeated for each pH pretreatment condition and each membrane type for SFU experiments.

A "best" pH pretreatment condition was selected based on SFU permeation results and additional factors explained in the discussion. This best pH pretreatment condition was then used for the RFU experiments, in which real urine was collected, pretreated to the best pH using the method described in Section 2.1, and pumped through a two-stage MF unit (SpectraPure), which consisted of a 1-µm sediment filter (L-SF-MT-1-10) and a 0.2-µm ZetaZorb sediment filter (L-SF-ZZ-0.2ABS-10), using a Cole-Parmer Masterflex peristaltic pump at 1000 mL/min. Pictures of the MF unit and pump can be seen in Figures S8 and S9. Ten liters of MF-pretreated RFU were added to the feed tank, and an undiluted urine sample, a t = 0 sample, and a permeate sample were all collected while running the system with the previous operating conditions. The pH and conductivity of samples were immediately measured, and samples were acidified with 12 M sulfuric acid (H_2SO_4) to below a pH of 2 to prevent further hydrolysis. Unfiltered samples were analyzed for TN and TOC. Samples were then filtered through nylon syringe filters with a pore size of 0.45 µm, and samples were analyzed for TAN, Cl^-, PO_4^{3-}, Na^+, K^+, Ca^{2+}, and Mg^{2+}; while SO_4^{2-} was measured for real urine samples, acidification of samples with H_2SO_4 prevented accurate membrane rejections of SO_4^{2-} to be calculated.

2.5. RO/NF Fouling Experiments

Fouling experiments were conducted to determine the effects of MF pretreatment on biological, organic, and inorganic fouling of the membranes. A “best” membrane was selected based on real and SFU permeation results and additional factors explained in the discussion. This best membrane was used for fouling experiments. A prewetted membrane was loaded into the membrane cell with a spacer in between its active side and the feed flow. Ten liters of DI water were added to the feed tank, and the system was run at previous operating conditions until the permeate flow was stable (approximately 4 h), signifying that the membrane was fully compacted. The DI water was drained from the feed tank. RFU was collected and pretreated to the predetermined best pH, and 10 L of urine without MF pretreatment were added to the feed tank. The system was run for 24 h at previous operating conditions, with the permeate looping back into the feed tank to ensure a constant urine concentration in the feed tank. Permeate flux data was measured every minute, and every 20 data points were averaged to show the long-term reduction in flux due to fouling. After the experiment, membranes were extracted from the membrane cell, and a small portion of the active area was cut and fixed in a glutaraldehyde solution at 4 °C for at least 1 h; the contents of the fixative solution can be seen in Table S3. After storage in the preservative, membranes were dehydrated using a series of incremented ethanol dilutions, from 0% to 100% ethanol in 20% increments, with each increment for at least 10 min. Membranes were then air-dried and analyzed using scanning electron microscopy (SEM) and Fourier-transformed infrared (FTIR). Importantly, it was not deemed necessary to conduct critical-point drying on the membranes, as the fixative method was able to sufficiently preserve biological molecules at the SEM resolution desired. The experiment was run in duplicate and was repeated with urine that was pretreated with MF. The method for MF pretreatment can be seen in Section 2.4.

2.6. Cleaning

Cleaning of the system was conducted in between experiments to remove biological, inorganic, and organic foulants from the insides of the membrane cell, tubing, pump, tank, and flow meters. For SFU experiments, the urine was drained from the feed tank, and the feed tank was rinsed with DI water. The membrane and spacer were taken out of the membrane cell, and the permeate tube was detached from the top of the membrane cell; a nut was attached in place of the permeate tube to cap the flow and provide backpressure for the system. The tank was then filled with 10 L of 0.05 mM ethylenedinitrilotetraacetic acid (EDTA) disodium salt dihydrate, and the system was run for at least 20 min at previous operating conditions. The tank was drained, rinsed with DI water, and filled with 10 L of a pH 11 solution prepared with 10 M NaOH (approximately 1.1 mL). The system was run for 10 min at previous operating conditions. The tank was drained, rinsed with DI water, and filled with 10 L of DI water. The system was run for 10 min at previous operating conditions, and the tank was drained.

For RFU experiments, the urine was drained from the feed tank, and the feed tank was rinsed with DI water. The membrane and spacer were taken out of the membrane cell, and the permeate tube was capped. The tank was filled with 10 L of DI water, and the system was run for 10 min at previous operating conditions to remove the residual urine in the system. The tank was drained, rinsed with DI water, and filled with 10 L of 10% bleach solution. The system was run for 30 min at previous operating conditions to inactivate any biological foulant residual in the system. The tank was drained, rinsed with DI water, and filled with EDTA disodium salt dihydrate solution. The previous cleaning cycle for the SFU experiments was then continued for the RFU experiments, i.e., EDTA disodium salt dihydrate, pH 11 solution, and DI water.

2.7. Economic Analysis

An economic analysis was conducted to illustrate different commercial products that could be created using recovered urea. Costs of commercial fertilizers were taken from Data Transmission Network/Progressive Farmer in February 2022 (Quinn, 2022). Costs of diesel exhaust fluid were taken from Discover DEF in March 2022 (*Discover DEF*, 2022). Costs were converted into cost per kg of nitrogen (N) for comparison. Other novel uses for urea were taken from previous literature.

2.8. Analytical Methods

Measurement of TOC and TN in unfiltered samples was conducted using Shimadzu TOC-L total organic carbon analyzer. Calibration standards for TOC were made using a potassium acid phthalate stock solution. Calibration standards for TN were made using a potassium nitrate stock solution. RICCA standards were used at TOC concentrations of 10 mg/L and 5 mg/L and at TN concentrations of 5 mg/L and 1 mg/L to check quality assurance.

Samples were filtered before analysis of ions through nylon syringe filters with a pore size of 0.45 µm. Measurement of ion concentrations (Cl^-, SO_4^{2-}, PO_4^{3-}, Na^+, K^+, Ca^{2+}, Mg^{2+}, and TAN) was conducted using flow injection analysis on an ion chromatography instrument, the Dionex ICS 5000+ (Sunnyvale, California). A 20 mM methanesulfonic acid eluent on a Dionex CS12A column was used for analysis of samples, at a suppression of 112 mA. A Dionex standard with ion concentrations was used to create a calibration curve for analysis. Peak analysis was conducted using Chromelon peak analysis version 7 software.

2.9. Data Analysis

Percent rejection was calculated by subtracting the feed (t = 0) concentration by the permeate concentration. Percent permeation was calculated by subtracting the percent rejection from 100%.

TN is represented by the combination of urea, NH_4^+, and NH_3. As stated before, TAN is represented as the combination of NH_4^+ and NH_3. For synthetic urine experiments, TN is expected to be made up of only urea; for real urine experiments, TAN is also expected to be in the urine in low concentrations, as urea hydrolysis cannot be completely inhibited in a real-world application of urine stabilization. The concentration of urea was thus calculated as the difference between TN and TAN concentrations.

Error was represented as standard deviation for this study. Error bars in figures represented the standard deviation of duplicate experiments for urea permeation, ion rejection, and TOC rejection. Letters over data bars show statistical significance groups, i.e., data bars marked with the same letter had no statistical differences, while data bars marked with different letters were statistically different. Statistical significance was determined using Two-Factor ANOVA tests and paired t-tests.

CHAPTER 3

RESULTS AND DISCUSSION

3.1. Evaluation of pH pretreatment conditions and membrane types for SFU

Three different pH pretreatment conditions (i.e., pH 5, 6, and 12) were evaluated to determine the efficacy of applying urine stabilization via acid or base addition before membrane treatment. Additionally, three different membrane types (i.e., BW30 RO, NF90, and NF270) were evaluated to identify the effects of membrane pore size on permeation of urea and rejection of other urine constituents. Figure 2 shows the permeation of urea for each of the pH pretreatment conditions and membrane types. As can be seen, there were minimal statistically differences between each pH condition for all three membrane types; only the NF270 showed a statistically significant difference between the pH 5 condition and the pH 6 and pH 12 conditions. However, in practice, the difference between 95.3% permeation (for pH 5 condition) versus 97-99% permeation (for pH 6 and pH 12 conditions) is minimal. Because urea is a neutrally charged compound, its rejection via membranes is dominated by size exclusion; electrostatic interactions, which are driven by the slight negative charge of RO and NF membranes, will have minimal effects on urea permeation. It is well-documented that increasing the solution pH increases the negative surface charge of a membrane (Childress & Elimelech, 1996), which could theoretically increase the rejection of urea due to the molecule's polar charge distribution; however, as can be seen by Figure 2, minimal significant differences between pH conditions can be observed, illustrating the relative insignificance of urea's polar charge distribution. It is important to note that in a RFU solution, the pH of solution could play a role in the urea permeation due to the presence of proteins; literature has shown that proteins have a negative charge at high pH and a positive charge at low pH (Shaw et al., 2001; Tanford, 1963), allowing for their rejection via electrostatic interactions by negatively charged membranes. The polarity of urea allows it to orient its nitrogen-hydrogen groups towards proteins for high pH solutions (or away from proteins for low pH solutions) (Chen et al., 2007); these additional interactions with proteins could result in higher rejection of urea above and below the average isoelectric point for the proteins in urine, but this is out of the scope of this study and thus was not investigated. Additionally, there were significant differences between different membrane conditions for all pH conditions. As membrane pore size increased (i.e., increasing from BW30 RO to NF270), urea permeation increased at all pH conditions, signifying the importance of membrane pore size on rejection of neutrally charged compounds. BW30 RO had the lowest average permeation of urea of 55%; NF90 had an average permeation of 77%; and NF270 had the highest average permeation of urea of 97%. These rejection trends are contradictory to what was found in previous literature, in which BW30 and NF90 in a dead-end orientation had no significant differences in urea rejection (Ray et al., 2020). Furthermore, urea permeation using NF90 was greater in this study than in previous literature that used a dead-end orientation (Ray et al., 2022). This improvement in permeation is significant, as it illustrates that a cross-flow orientation not only has improved lifetime (i.e., due to formation of a "gel-layer" foulant rather than a "cake-layer" foulant) but also has improved performance. Furthermore, the low rejection of urea by NF270 was comparable to previous literature, in which neutrally charged, polar organic compounds were rejected poorly by NF270 (Breitner, 2017). Notably, previous literature found that polyamide membranes such as the three used in this study had higher rejection of neutrally charged, polar compounds than membranes made with different materials, such as cellulose acetate (Fang & Chian, 1976). Polyamide membranes were selected for this study due to their common application for full-scale membrane treatment, but it may be beneficial to apply other membranes, such as cellulose acetate membranes, for recovery of urea.

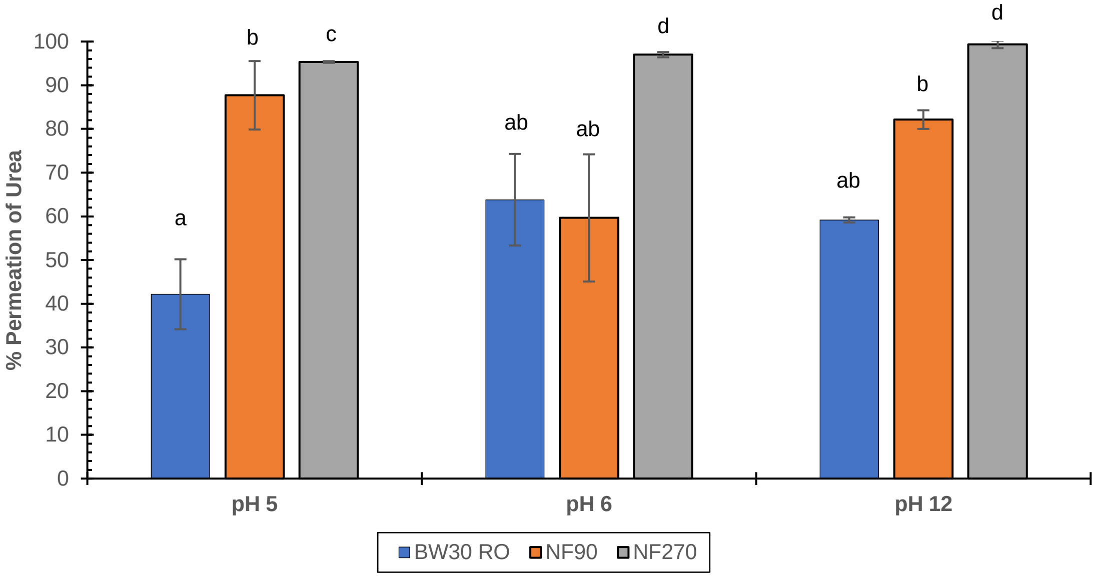

Figure 2. Urea permeation results for SFU experiments, across three pH pretreatment conditions and three membranes.

Figure 3 shows the rejection of conductivity for each of the pH pretreatment conditions and membrane types. As can be seen, there were minimal statistical differences across different pH conditions, besides for NF270, in which higher pH resulted in higher rejection of ions. As stated before, previous literature has shown that an increase in solution pH increases the negative surface charge of the membrane (Childress & Elimelech, 1996). While for BW30 RO and NF90, the pore size is sufficiently small enough that this surface charge difference has negligible effects, the larger pore size of NF270 resulted in fewer ions being rejected via size exclusion and a more significant contribution of rejection via electrostatic interactions. Thus, the highly negative surface charge of NF270 at pH 12 allowed for a significant increase in ion rejection compared to lower pH conditions. Additionally, there were no significant differences in conductivity rejection between BW30 RO and NF90 at each pH condition. This signifies the advantages of NF90 over BW30 RO; while the two membranes have comparable ion rejections, NF90 had significantly higher permeation of urea. Thus, NF90 could be used to create a more pure concentrated urea product than BW30 RO. These results are different from previous literature in a dead-end orientation, which showed that there were no significant differences in urea permeation or conductivity rejection (Ray et al., 2020). Notably, while the timescales of these experiments may not have been enough to form a visible fouling layer, molecular-scale interactions could have caused a reduction in effective pore size enough to see differences between dead-end and cross-flow filtration. In any case, this is out of the scope of this study and requires future work. Lastly, the NF270 had low conductivity rejection for all three pH conditions. As stated above, the increase in pore size resulted in lowered rejection of all compounds.

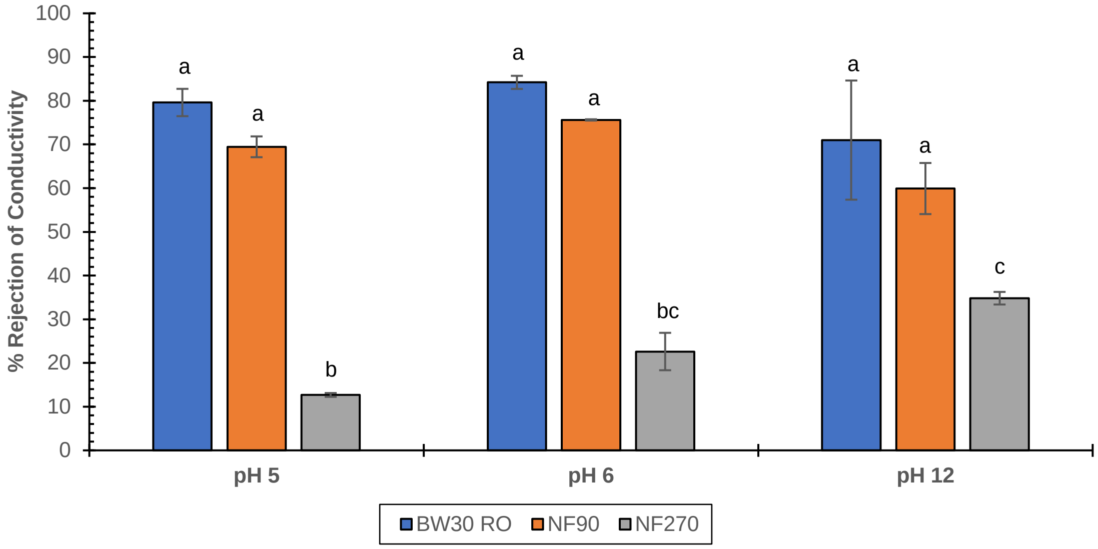

Figure 3. Conductivity rejection results for SFU experiments, across three pH pretreatment conditions and three membranes.

Figure 4 shows the specific rejections of ions for (a) BW30 RO, (b) NF90, and (c) NF270. As can be seen, no significant differences between specific ion rejections were seen for BW30 RO. For NF90, the majority of conditions had no significant differences besides a lower rejection of monovalent ions (i.e., Cl^- and Na^+) at pH 12 than phosphate at pH 5. However, for NF270, multivalent ions (i.e., SO_4^{2-} and PO_4^{3-}) had a significantly higher rejection than monovalent ions. The minimal significant differences between ions for BW30 RO and NF90 illustrate the importance of pore size for these membranes. While electrostatic interactions alone would result in greater rejection of multivalent ions, the small pore sizes of BW30 RO and NF90 allow for high rejection of monovalent at comparable rates as multivalent ions. However, for NF270, two reasons can be attributed to the higher rejection of multivalent ions than monovalent ions: firstly, the multivalent ions measured in this study are multiatomic and have larger molecular weights than monovalent ions, resulting in greater size exclusion of these ions; secondly, a higher charge for multivalent ions results in greater electrostatic forces between ions and the membrane surface, resulting in greater electrostatic rejection of these ions. NF270 membranes have been well-documented within literature to have high rejection of multivalent anions via Donnan exclusion (Donnan, 1995; Li et al., 2018; Wu et al., 2016) but low rejection of monovalent ions (Aher et al., 2017; Boo et al., 2018; Kammoun et al., 2020; Li et al., 2018).

Given the high permeation of urea and rejection of multivalent ions, NF270 could be used for selective separation of urea and monovalent ions from multivalent ions. However, given other available methods to separate multivalent ions from urine, e.g., precipitation via pH adjustment(Randall et al., 2016), it is likely not economically favorable to treat urine via NF270. Given that there were minimal significant differences observed between the three pH conditions, the pH 5 condition was selected as the “best” pH condition for two reasons: (a) pH 6 cannot be used in a real-world system, as urine stabilization is necessary for recovery of urea and to reduce operational challenges associated with urine collection (Z. Liu et al., 2008; Ohki et al., 2010; Ray et al., 2018; Udert, Larsen, et al., 2003); (b) pH 5 is preferred over pH 12, as pH 12 is greater than the commercially-specified pH operating conditions, and high pH solutions have been shown to cause reduced membrane performance (Dalwani et al., 2011).

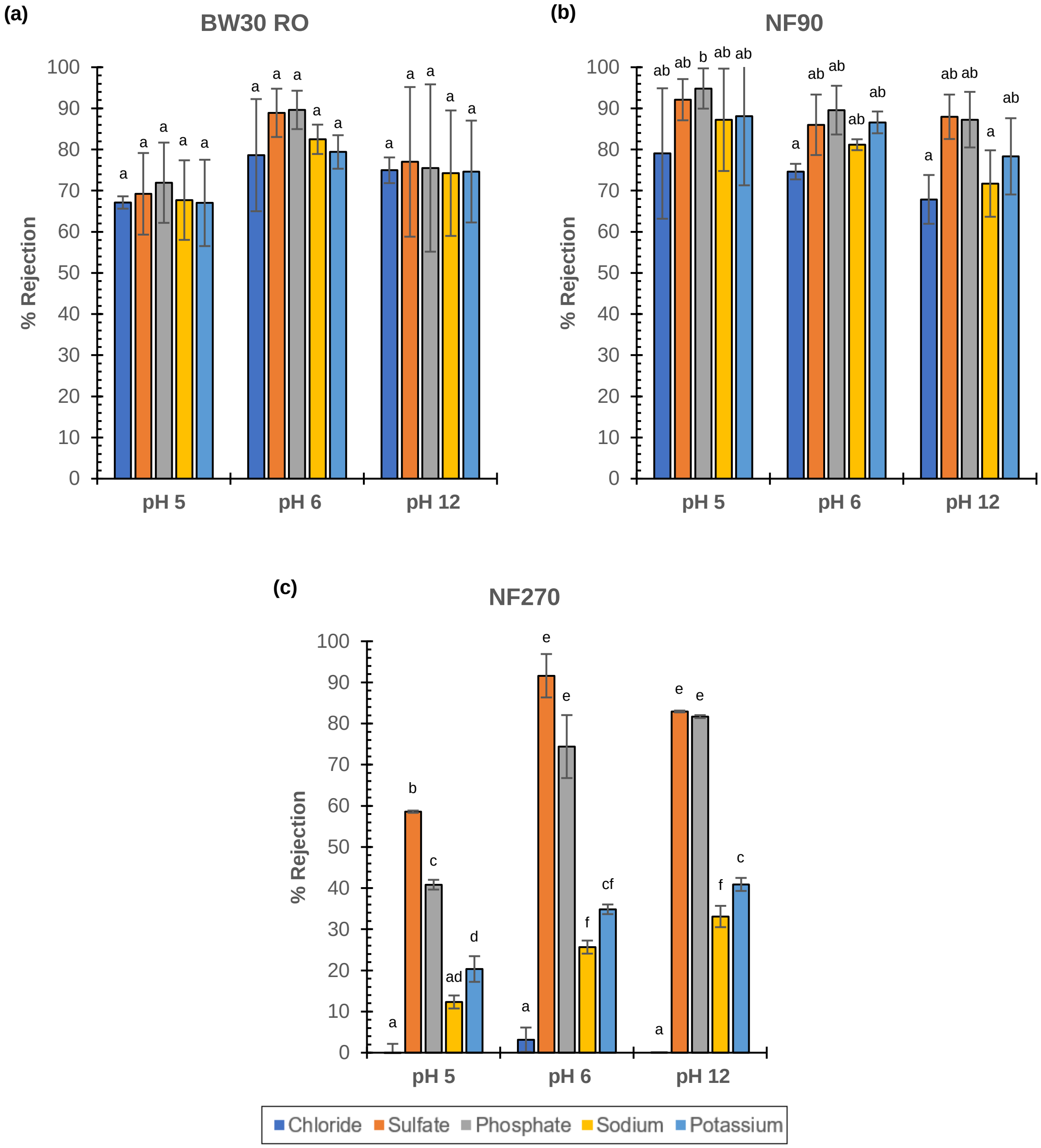

Figure 4. Specific ion rejection results for SFU experiments, across three pH pretreatment conditions and two membranes: **(a)** BW30 RO, **(b)** NF90, and **(c)** NF270.

3.2. Comparison of RFU with SFU for best pH condition

Urea permeation experiments were conducted using RFU to determine the efficacy of recovering urea from fresh human urine in a real-world system. The “best” pH condition identified from SFU experiments were used (i.e., pH 5). Figure 5 shows the rejection of different compounds from RFU at pH 5 by the three membranes. As can be seen, NF90 performed favorably to BW30 for most constituents, i.e., lower rejection (higher permeation) of urea but comparable rejection of ions, though it did have a significantly lower rejection of TOC. Furthermore, NF270 had similar trends to synthetic urine experiments, with a high (>94%) permeation of urea but a low rejection of monovalent ions; phosphate, a multivalent ion, was rejected with >77% efficiency by NF270. These results signify the efficacy of NF90 to produce a urea product in a real-world system, although concerns over organic constituents, such as microorganisms or proteins, could justify the use of BW30 RO over NF90 in specific applications.

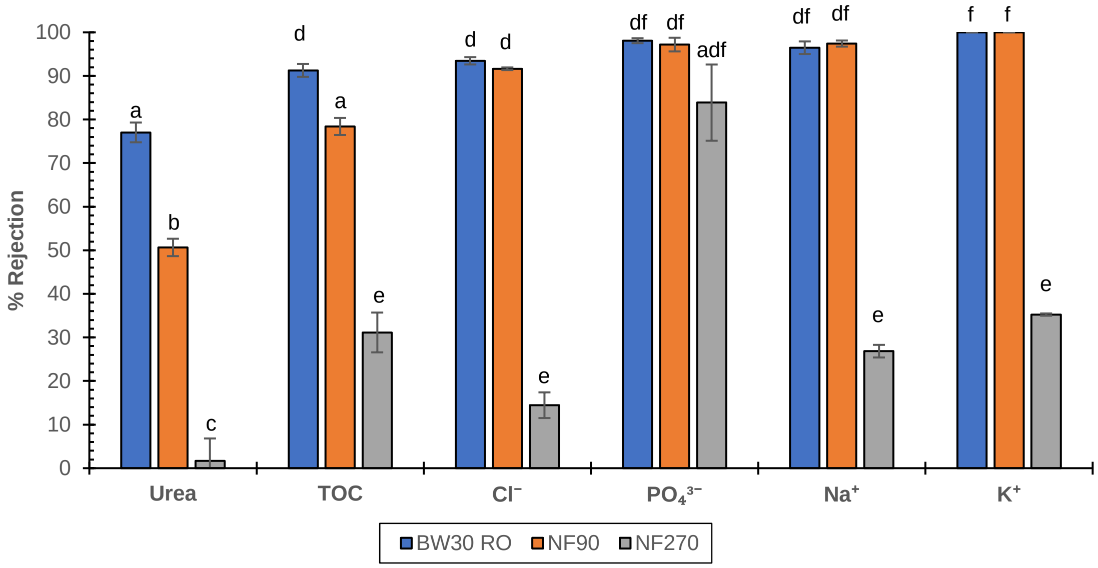

Figure 5. Rejection of different compounds by BW30 RO, NF90, and NF270, from RFU.

Figure 6 shows a comparison between SFU results and RFU results for the pH 5 condition. As can be seen, the rejection from real urine was higher for NF90 experiments (i.e., the permeation was lower), but similar trends existed, where the NF90 performed favorably to BW30 and NF270 had high urea permeation and low conductivity rejection. These results suggest additional rejection of constituents due to organics existing in real urine (e.g., microorganisms, proteins), which may have contributed to molecular-scale reduction of the effective pore size of the membranes; however, this reduction was only produced a statistical difference for NF90, signifying that membranes with too large of a pore size (i.e., NF270) will not have a reduction in effective pore size that is significant enough to reject more ions by size exclusion, but membranes with too small of a pore size (i.e., BW30 RO) will already have a small enough pore size that the constituents are already being rejected at high rates and the additional reduction in effective pore size does not produce a significant difference in rejection. While there were no statistically significant differences for BW30 and NF270 between SFU and RFU in these experiments, there does appear to be greater rejection from RFU than SFU based on visual results; it could feasibly be hypothesized that with additional experiments, the reduction in effective pore size will produce statistically significant differences between RFU and SFU experiments.

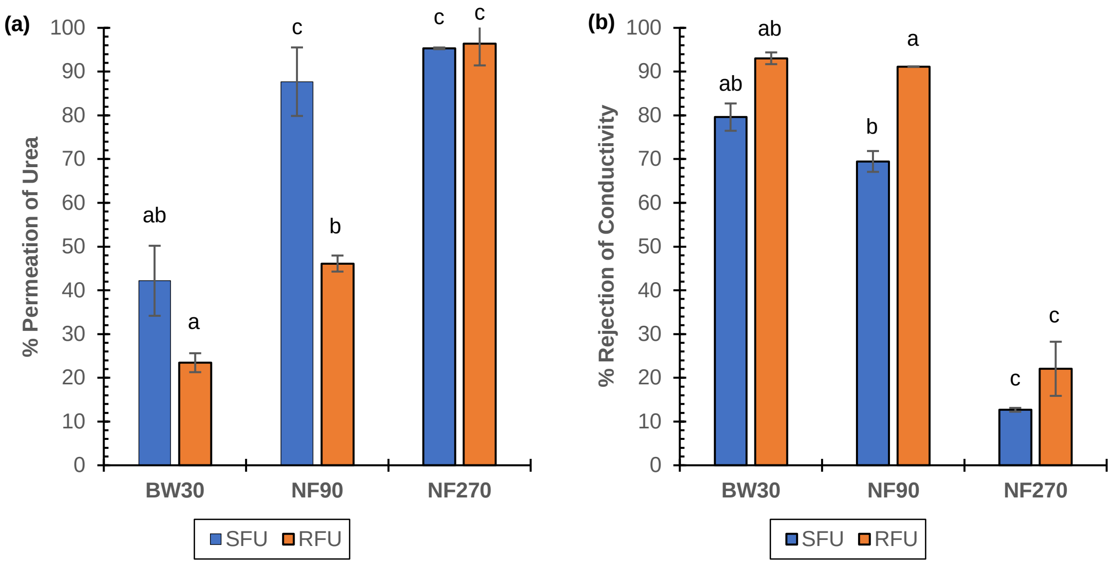

Figure 6. Comparison of SFU and RFU experiments for (a) urea permeation and (b) conductivity rejection.

Given its significantly higher permeation of urea but comparable ion rejection to BW30 RO, NF90 was selected as the "best" membrane for producing a pure urea product. As stated before, NF270 is likely not economically competitive to other processes that separate multivalent ions from other urine constituents.

3.3. Fouling mitigation with MF pretreatment

Fouling experiments were conducted to characterize fouling of membranes in a cross-flow orientation during membrane treatment of RFU and determine if MF pretreatment can be a suitable mitigation strategy. The "best" condition from Sections 3.1 and 3.2 was used for fouling experiments (i.e., NF90, pH 5 RFU). Permeate flow reduction for MF and no-MF conditions over the 24 h period can be seen in Figure 7. Duplicate results for permeate flow can be seen in Figure S10. Pictures of the membranes after the 24 h period can be seen in Figure 8. As can be seen, a thicker foulant was produced during the experiment without MF pretreatment. This corresponded to a more significant permeate flow reduction, showing the operational benefits of including MF pretreatment of urine before membrane treatment.

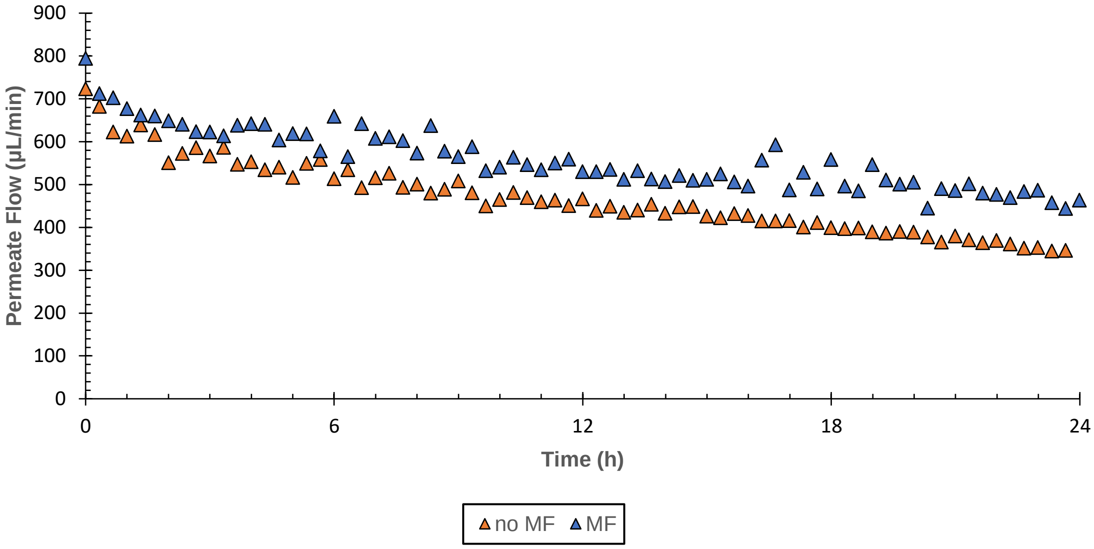

Figure 7. Permeate flow reduction over the 24 h period for experiments with and without MF pretreatment.

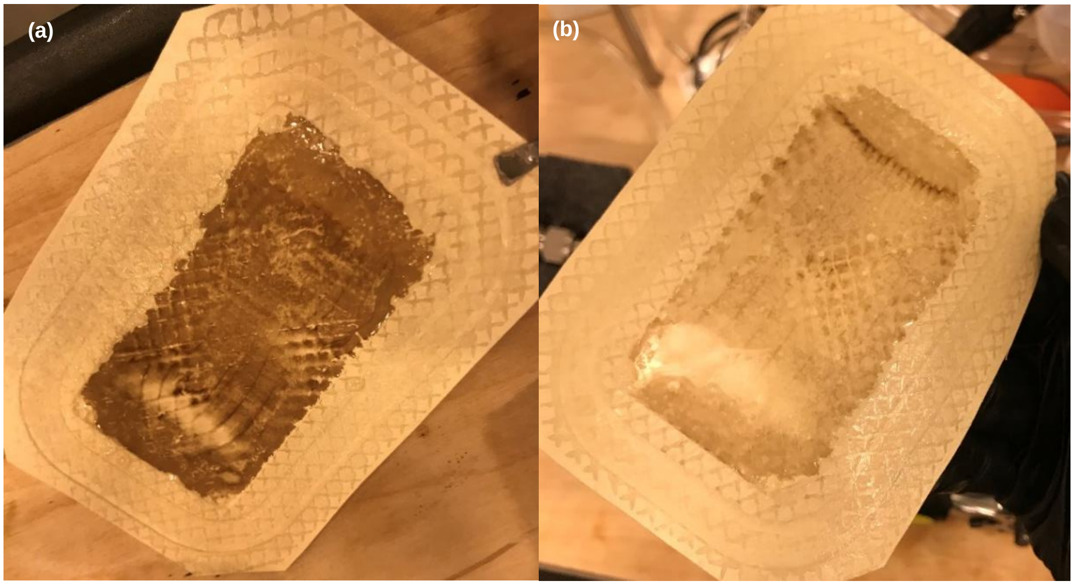

Figure 8. Fouled membranes after 24 h experiments, with (a) no MF pretreatment and (b) MF pretreatment.

FTIR analysis results can be seen in Figure 9. Notably, the gel-layer foulant was loosely attached to the membrane, resulting in significant detachment of the foulant during preservation of the foulant for SEM and FTIR analysis, especially for experiments with no MF pretreatment. Even with this significant detachment, the results of FTIR showed greater peak suppression (i.e., at 3300 cm^{-1}) for experiments with no MF pretreatment, signifying that the foulant still attached was thicker than that of fouled membranes with MF pretreatment. Importantly, at low wavenumbers (i.e., high wavelengths), high transmittance peaks could be seen that were greater than that of the virgin NF90 membrane; these high peaks may have been due to ethanol dehydration of membranes for foulant preservation, which may have left residual ethanol on the surface of the membranes.

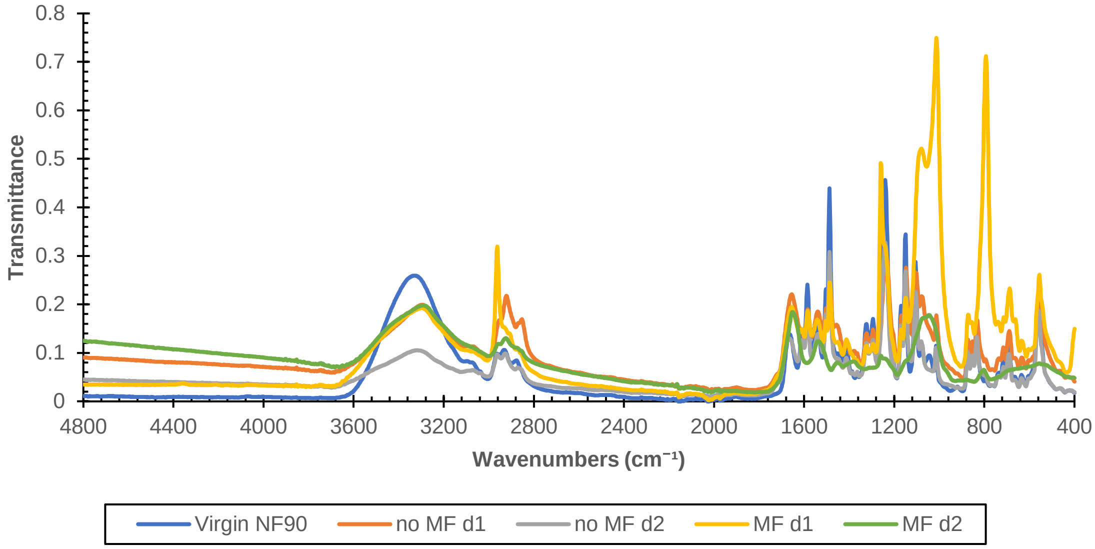

Figure 9. FTIR analysis results for two treatment conditions, with duplicates, compared to virgin NF90 membrane.

Figure 10 shows SEM imagery of the virgin NF90 membrane. As can be seen, the virgin membrane has minor imperfections, such as scratches and precipitate, that could result in loss in performance and provide binding sites for microorganisms in the foulant. Additionally, precipitate on the surface can block pores and reduce the effective pore size of unfouled membrane.

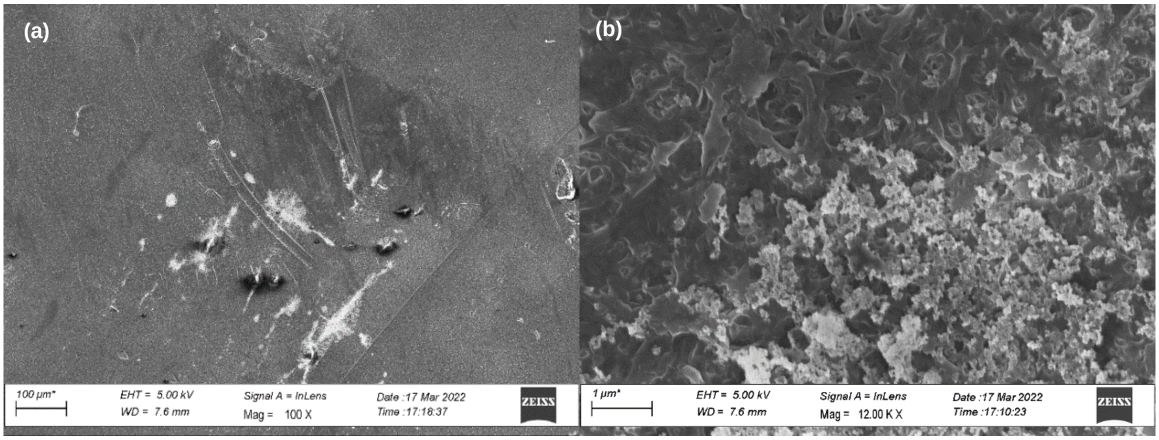

Figure 10. SEM imagery of virgin NF90 membrane, at (a) 100-times magnification and (b) 28,000-times magnification.

Figure 11 shows SEM imagery of the fouled membranes for experiments with no MF pretreatment. As seen, in areas where the foulant did not detach, a dense layer of microorganisms could be seen, made up mostly of rod-shaped or spherical bacteria (as seen in (a) through (c)). Based on previous literature, these bacteria are likely *Enterobacteriales* or *Lactobacillales* that were abundant in urine treated with acetic acid (Saetta et al., 2020). Additionally, as seen in (d), clustering of microorganisms and precipitation occurred along imperfections in the membrane, even after a large majority of the foulant detached from the membrane. Reduction of fouling along these imperfections would likely require chemical cleaning.

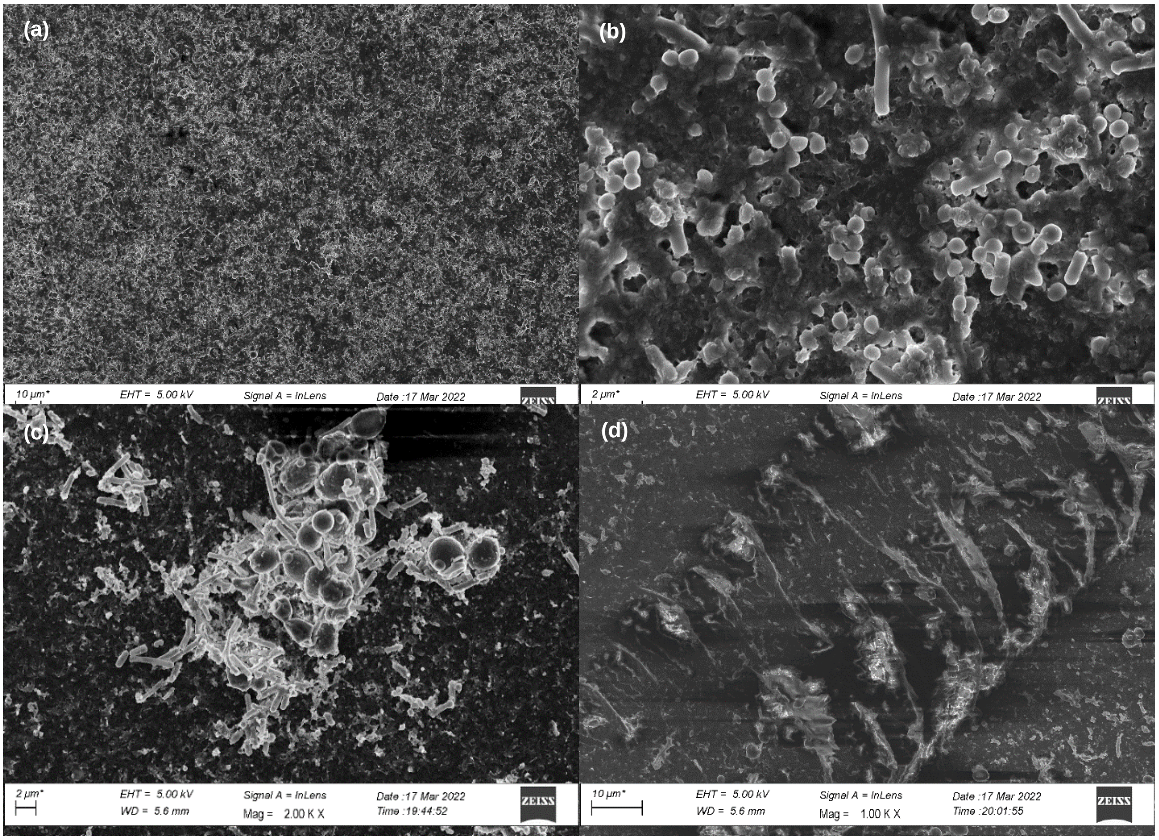

Figure 11. SEM imagery of biofouled NF90 membrane for experiments with no MF pretreatment, for duplicate 1 at (a) 500-times magnification and (b) 5,000-times magnification; and for duplicate 2 at (c) 2,000-times magnification and (d) 1,000-times magnification.

Figure 12 shows SEM imagery of the fouled membranes for experiments with MF pretreatment. As can be seen, on a molecular scale, the density of foulant was comparable in some areas to that of experiments with no MF pretreatment, though this may be attributed to detachment of the foulant during membrane fixation. However, based on visual confirmation, there appear to be fewer larger rod-shaped bacteria (likely *Lactobacillales*), signifying removal of these larger microorganisms by MF. Notably, for both experimental conditions, smaller proteins were abundant on the surface of the microorganisms; these proteins could feasibly be small enough to partially pass through the membrane, contributing to the lowered rejection of TOC observed in RFU experiments. Previous literature has shown low rejection of small proteins and amino acids by nanofiltration membranes (Cao et al., 2021). Thus, urea-based products made with membrane-recovered urea may require additional considerations to account for proteins and other small, organic material that may permeate through the membrane.

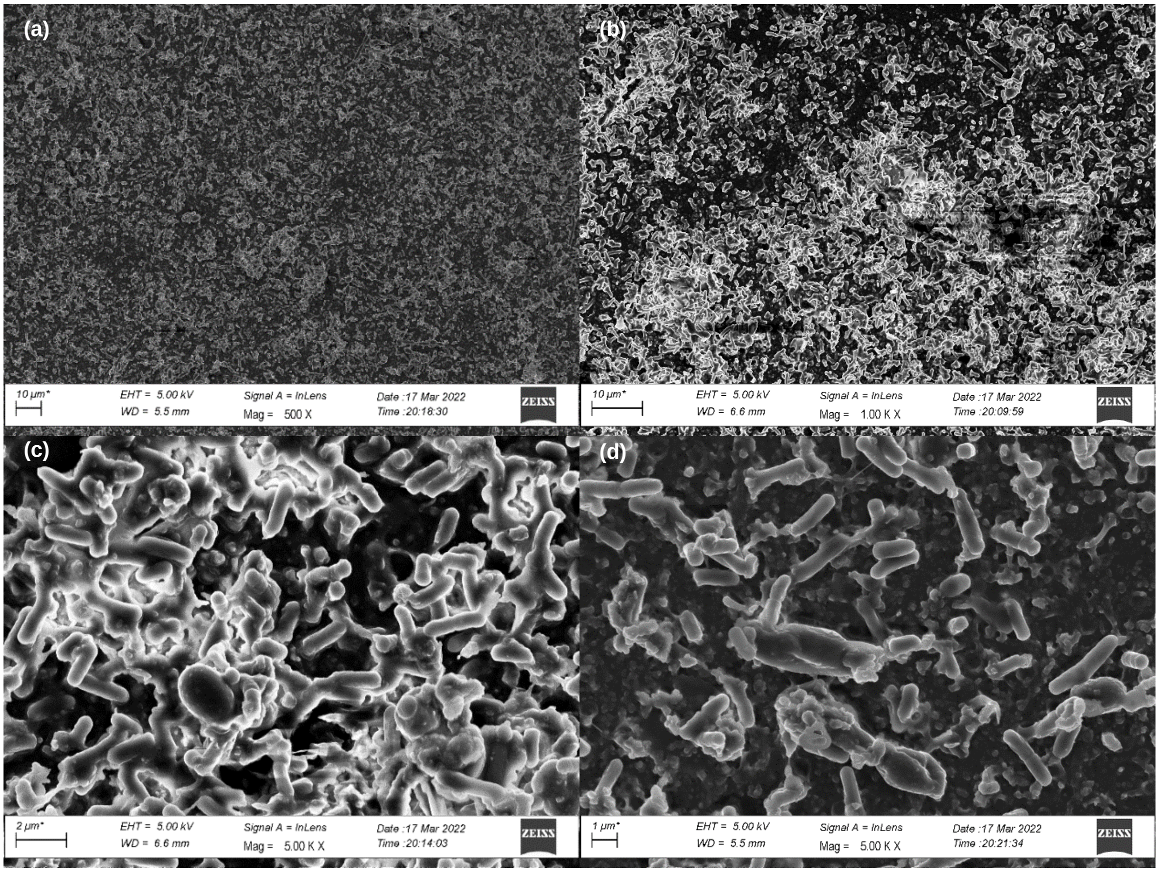

Figure 12. SEM imagery of biofouled NF90 membranes for experiments with MF pretreatment, for duplicate 1 at (a) 500-times magnification, (b) 1,000-times magnification, and (c) 5,000-times magnification; for duplicate 2 at (d) 5,000-times magnification.

Based on the permeate flux reduction results, FTIR results, and SEM imagery, it can be seen that MF pretreatment successfully reduces the fouling of NF90 for the purpose of urea recovery from RFU. However, previous results also showed that RFU had greater rejection of urine constituents than SFU, producing a more pure but less concentrated urea product; this was likely due to the additional organic and biological foulants in RFU. Thus, it may be beneficial for certain applications to allow for buildup of a fouling layer before collection of the permeate to produce a more pure urea product due to reduction of the effective pore size of the membrane. Importantly, applying MF pretreatment did not completely reduce fouling of the membrane, signifying the potential for long-term operation of the membrane system to produce a highly pure urea product.

3.4. Economic analysis of different urea-based products

Urea recovered from RFU could be used for a multitude of products, including different commercial fertilizers, commercial diesel exhaust fluid, urea-based ion exchange resins, biocement, and synthetic polymers. A summary of commercially available urea-based products and comparable products can be seen in Table 1. As can be seen, the most expensive fertilizers on the market include phosphate. When comparing nitrogen-based fertilizers only, urea-based fertilizers are not economically competitive with anhydrous ammonia in the current market on a normalized basis. Thus, creating these urea-based fertilizers, as well as diesel exhaust fluid, from recovered urea could greatly reduce the overall price of these fertilizers. Furthermore, given the current shortages of urea and fluctuations in fertilizer prices in the world market (Quinn, 2022; Zhong, 2021), implementing urea recovery from urine could have major impacts for food production and other urea applications.

Table 1

Different commercially available urea-based products.

Product Category	Product	Cost per ton	Cost per kg N
Fertilizers (Quinn, 2022)	Diammonium phosphate (DAP)	$874/ton	$4.54/kg N
	Monoammonium phosphate (MAP)	$935/ton	$8.46/kg N
	Anhydrous ammonia	$1,488/ton	$1.25/kg N
	Urea-ammonium-nitrate-28 (UAN-28)	$603/ton	$2.37/kg N
	UAN-32	$703/ton	$2.08/kg N
	Urea	$891/ton	$2.21/kg N
Other	Diesel exhaust fluid (DEF) (*Discover DEF*, 2022)	$642/ton	$4.67/kg N

While commercially available products have set worldwide markets, other urea-based products not commercially available could be valuable in the future. For example, urea-based ion exchange resins have been developed that have high selectivity for metals (Jadhao et al., 2005; Jadhao et al., 2009); urine-recovered urea has been used for alternative biocementation processes such as microbial-induced carbonate precipitation (Henze & Randall, 2018; Lambert & Randall, 2019) and enzyme-induced carbonate precipitation (Crane et al., 2022); and urea has been used as a building block for production of synthetic elastomers (M. Chen et al., 2018; Sirrine et al., 2018) and urea-formaldehyde adhesive resins (Conner, 1996). Many of these novel urea-based materials are only in experimental stages of development, but future production of these materials using urine-recovered urea could allow for significant reduction of costs for these processes.

CHAPTER 4

CONCLUSION

This study examined the efficacy of urea recovery from RFU using membrane treatment. The following major conclusions were found in the study.

- NF90 membrane had advantageous performance to BW30 RO and NF270, allowing for production of a pure urea product from fresh urine.
- Urea stabilization via acetic acid addition did not inhibit membrane performance, signifying that fresh urine pretreatment to pH 5 could be used as an optimum pH condition for urea recovery from RFU.
- RFU experiments had higher rejection of urine constituents than SFU, signifying that organic constituents in RFU reduce the effective pore size of membranes.
- Pretreatment of urine with MF reduced the thickness of the foulant, resulting in lowered permeate flow loss and a longer lifetime.

Practical application of membrane treatment of urine would include a multi-step process to optimize urine collection, stabilization, and treatment. Collection of urine on a system-scale, such as in a building collection system (Boyer & Saetta, 2019; N. S. Jagtap & Boyer, 2020; Saetta et al., 2019), could occur using waterless urinals (*WES-4000 | Sloan*, n.d.) or urine-diverting toilets (*Save! | Design & Innovation*, n.d.). At the point of use, acid or base addition could be applied in doses high enough to inhibit the ureolysis process throughout the collection system and in the storage system (Randall et al., 2016; Ray et al., 2018; Saetta et al., 2020). Collected urine could then undergo different treatment steps to selectively recover different nutrients: e.g., membrane treatment could be used to recover urea, chemical precipitation could be used to recover phosphate (Guan et al., 2020; Pradhan et al., 2017; J. A. Wilsenach et al., 2007), and adsorption could be used to recover pharmaceutical compounds (Solanki & Boyer, 2017). Recovered urea could then be used to produce fertilizers, biocement, or synthetic polymers.

REFERENCES

Aher, A., Papp, J., Colburn, A., Wan, H., Hatakeyama, E., Prakash, P., Weaver, B., & Bhattacharyya, D. (2017). Naphthenic acids removal from high TDS produced water by persulfate mediated iron oxide functionalized catalytic membrane, and by nanofiltration. *Chemical Engineering Journal, 327*. https://doi.org/10.1016/j.cej.2017.06.128

Antonini, S., Paris, S., Eichert, T., & Clemens, J. (2011). Nitrogen and Phosphorus Recovery from Human Urine by Struvite Precipitation and Air Stripping in Vietnam. *CLEAN – Soil, Air, Water, 39*(12), 1099–1104. https://doi.org/10.1002/clen.201100036

Başakçilardan-Kabakci, S., İpekoğlu, A. N., & Talinli, I. (2007). Recovery of Ammonia from Human Urine by Stripping and Absorption. *Environmental Engineering Science*, *24*(5), 615–624. https://doi.org/10.1089/ees.2006.0412

Boerner, L. K. (2019, June 15). *Industrial ammonia production emits more CO_2 than any other chemical-making reaction. Chemists want to change that*. Chemical & Engineering News. https://cen.acs.org/environment/green-chemistry/Industrial-ammonia-production-emits-CO2/97/i24

Boo, C., Wang, Y., Zucker, I., Choo, Y., Osuji, C. O., & Elimelech, M. (2018). High Performance Nanofiltration Membrane for Effective Removal of Perfluoroalkyl Substances at High Water Recovery. *Environmental Science & Technology*, *52*(13), 7279–7288. https://doi.org/10.1021/acs.est.8b01040

Bowen, W. R., Mohammad, A. W., & Hilal, N. (1997). Characterisation of nanofiltration membranes for predictive purposes—Use of salts, uncharged solutes and atomic force microscopy. *Journal of Membrane Science*, *126*(1), 91–105. https://doi.org/10.1016/S0376-7388(96)00276-1

Boyer, T. H., & Saetta, D. (2019). Opportunities for Building-Scale Urine Diversion and Challenges for Implementation. *Accounts of Chemical Research*, *52*(4), 886–895. https://doi.org/10.1021/acs.accounts.8b00614

Breitner, L. N. (2017). *REJECTION OF LOW MOLECULAR WEIGHT NEUTRAL ORGANICS BY REVERSE OSMOSIS MEMBRANES FOR POTABLE REUSE* [Thesis].

Cao, Y., Chen, G., Wan, Y., & Luo, J. (2021). Nanofiltration membrane for bio-separation: Process-oriented materials innovation. *Engineering in Life Sciences*, *21*(6), 405–416. https://doi.org/10.1002/elsc.202000100

Chen, M., Inglefield, D. L., Zhang, K., Hudson, A. G., Talley, S. J., Moore, R. B., & Long, T. E. (2018). Synthesis of urea-containing ABA triblock copolymers:

Influence of pendant hydrogen bonding on morphology and thermomechanical properties. *Journal of Polymer Science Part A: Polymer Chemistry*, *56*(16), 1844–1852. https://doi.org/10.1002/pola.29066

Chen, X., Sagle, L. B., & Cremer, P. S. (2007). Urea Orientation at Protein Surfaces. *Journal of the American Chemical Society*, *129*(49), 15104–15105. https://doi.org/10.1021/ja075034m

Childress, A. E., & Elimelech, M. (1996). Effect of solution chemistry on the surface charge of polymeric reverse osmosis and nanofiltration membranes. *Journal of Membrane Science*, *119*(2), 253–268. https://doi.org/10.1016/0376-7388(96)00127-5

Christiaens, M. E. R., De Paepe, J., Ilgrande, C., De Vrieze, J., Barys, J., Teirlinck, P., Meerbergen, K., Lievens, B., Boon, N., Clauwaert, P., & Vlaeminck, S. E. (2019). Urine nitrification with a synthetic microbial community. *Systematic and Applied Microbiology*, *42*(6), 126021. https://doi.org/10.1016/j.syapm.2019.126021

Conner, A. H. (1996). UREA-FORMALDEHYDE ADHESIVE RESINS*. *Polymeric Materials Encyclopedia*, *11*, 8.

Courtney, C., & Randall, D. G. (2022). Concentrating stabilized urine with reverse osmosis: How does stabilization method and pre-treatment affect nutrient recovery, flux, and scaling? *Water Research*, *209*, 117970. https://doi.org/10.1016/j.watres.2021.117970

Crane, L., Ray, H., Hamdan, N., & Boyer, T. H. (2022). Enzyme-Induced Carbonate Precipitation Utilizing Fresh Urine and Calcium-Rich Zeolites. *Journal of Environmental Chemical Engineering*, 107238. https://doi.org/10.1016/j.jece.2022.107238

Dalwani, M., Benes, N., Bargeman, G., Stamatialis, D., & Wessling, M. (2011). Effect of pH on the performance of polyamide/polyacrylonitrile based thin film composite membranes. *Journal of Membrane Science*, *372*, 228–238. https://doi.org/10.1016/j.memsci.2011.02.012

Discover DEF. (2022). https://www.discoverdef.com/

Donnan, F. G. (1995). Theory of membrane equilibria and membrane potentials in the presence of non-dialysing electrolytes. A contribution to physical-chemical physiology. *Journal of Membrane Science*, *100*(1), 45–55. https://doi.org/10.1016/0376-7388(94)00297-C

Dow Filmtec Membranes | Flat Sheet Membrane Chart. (n.d.). LennTech. Retrieved March 25, 2022, from https://www.lenntech.com/Data-sheets/Filmtec-Flat-Sheet-Membrane-Chart-L.pdf

Fang, H. H. P., & Chian, E. S. K. (1976). Reverse osmosis separation of polar organic compounds in aqueous solution. *Environmental Science & Technology*, *10*(4), 364–369. https://doi.org/10.1021/es60115a011

Feng, D., Wu, Z., & Xu, S. (2008). Nitrification of human urine for its stabilization and nutrient recycling. *Bioresource Technology*, *99*(14), 6299–6304. https://doi.org/10.1016/j.biortech.2007.12.007

Ganrot, Z., Dave, G., & Nilsson, E. (2007). Recovery of N and P from human urine by freezing, struvite precipitation and adsorption to zeolite and active carbon. *Bioresource Technology*, *98*(16), 3112–3121. https://doi.org/10.1016/j.biortech.2006.10.038

Guan, T., Kuang, Y., Li, X., Fang, J., Fang, W., & Wu, D. (2020). The recovery of phosphorus from source-separated urine by repeatedly usable magnetic Fe3O4@ZrO2 nanoparticles under acidic conditions. *Environment International*, *134*, 105322. https://doi.org/10.1016/j.envint.2019.105322

Henze, J., & Randall, D. G. (2018). Microbial induced calcium carbonate precipitation at elevated pH values (>11) using Sporosarcina pasteurii. *Journal of Environmental Chemical Engineering*, *6*(4), 5008–5013. https://doi.org/10.1016/j.jece.2018.07.046

Hug, A., & Udert, K. M. (2013). Struvite precipitation from urine with electrochemical magnesium dosage. *Water Research*, *47*(1), 289–299. https://doi.org/10.1016/j.watres.2012.09.036

Jadhao, M. M., Paliwal, L. J., & Bhave, N. S. (2009). Ion-exchange properties of 2,2'-dihydroxybiphenyl—Urea—Formaldehyde terpolymer resins. *Desalination*, *247*(1), 456–465. https://doi.org/10.1016/j.desal.2008.07.020

Jadhao, M., Paliwal, lalitmohan, & Bhave, N. (2005). Chelation ion-exchange properties of 2,2′-dihydroxybiphenyl-urea- formaldehyde (2:1:3) resin. *Indian Journal of Chemistry - Section A Inorganic, Physical, Theoretical and Analytical Chemistry*, *44*, 1206–1210.

Jagtap, N., & Boyer, T. H. (2018). Integrated, multi-process approach to total nutrient recovery from stored urine. *Environmental Science: Water Research & Technology*, *4*(10), 1639–1650. https://doi.org/10.1039/C8EW00004B

Jagtap, N. S., & Boyer, T. H. (2020). Urine collection in a multi-story building and opportunities for onsite recovery of nutrients and non-potable water. *Journal of Environmental Chemical Engineering*, *8*(4). https://doi.org/10.1016/j.jece.2020.103964

Kammoun, M. A., Gassara, S., Palmeri, J., Ben Amar, R., & Deratani, A. (2020). Nanofiltration performance prediction for brackish water desalination: Case study of Tunisian groundwater. *DESALINATION AND WATER TREATMENT*, *181*, 27–39. https://doi.org/10.5004/dwt.2020.25100

King, R. E. (2021, December 12). *Global Urea Shortage Could Park Diesel Trucks*. https://jalopnik.com/global-urea-shortage-could-park-diesel-trucks-1848201479

Kistiakowsky, G. B., & Rosenberg, A. J. (1952). The Kinetics of Urea Hydrolysis by Urease. *Journal of the American Chemical Society*, *74*(20), 5020–5025. https://doi.org/10.1021/ja01140a009

Lambert, S. E., & Randall, D. G. (2019). Manufacturing bio-bricks using microbial induced calcium carbonate precipitation and human urine. *Water Research*, *160*, 158–166. https://doi.org/10.1016/j.watres.2019.05.069

Li, K., Ma, W., Han, H., Xu, C., Han, Y., Wang, D., Ma, W., & Zhu, H. (2018). Selective recovery of salt from coal gasification brine by nanofiltration membranes. *Journal of Environmental Management*, *223*, 306–313. https://doi.org/10.1016/j.jenvman.2018.06.032

Lind, B.-B., Ban, Z., & Bydén, S. (2000). Nutrient recovery from human urine by struvite crystallization with ammonia adsorption on zeolite and wollastonite. *Bioresource Technology*, *73*(2), 169–174. https://doi.org/10.1016/S0960-8524(99)90157-8

Liu, B., Giannis, A., Zhang, J., Chang, V. W.-C., & Wang, J.-Y. (2015). Air stripping process for ammonia recovery from source-separated urine: Modeling and optimization. *Journal of Chemical Technology and Biotechnology*, *90*(12), 2208–2217. Scopus. https://doi.org/10.1002/jctb.4535

Liu, Z., Zhao, Q., Wang, K., Lee, D., Qiu, W., & Wang, J. (2008). Urea hydrolysis and recovery of nitrogen and phosphorous as MAP from stale human urine. *Journal of Environmental Sciences*, *20*(8), 1018–1024. https://doi.org/10.1016/S1001-0742(08)62202-0

Murkes, J., & Carlsson, C.-G. (1988). *Crossflow filtration: Theory and practice*. Wiley.

Ohki, T., Nishikawa, N., Hasegawa, T., Okano, T., & Tanizawa, Y. (2010). Characterization of Scale Formed on the Surfaces of Toilet Bowls. *Journal of Surfactants and Detergents*, *13*(1), 19–26. https://doi.org/10.1007/s11743-009-1147-1

Patel, P. (2020, June 18). *One-step synthesis of urea could green up the fertilizer's act*. Chemical & Engineering News. https://cen.acs.org/synthesis/One-step-synthesis-urea-green/98/i24

Pradhan, S. K., Mikola, A., & Vahala, R. (2017). Nitrogen and Phosphorus Harvesting from Human Urine Using a Stripping, Absorption, and Precipitation Process.

Environmental Science & Technology, *51*(9), 5165–5171. https://doi.org/10.1021/acs.est.6b05402

Pronk, W., Palmquist, H., Biebow, M., & Boller, M. (2006). Nanofiltration for the separation of pharmaceuticals from nutrients in source-separated urine. *Water Research*, *40*, 1405–1412. https://doi.org/10.1016/j.watres.2006.01.038

Quinn, R. (2022a, February 23). *Most Fertilizer Prices Continue Upward Climb*. DTN Progressive Farmer. https://www.dtnpf.com/agriculture/web/ag/news/crops/article/2022/02/23/fertilizer-prices-continue-upward

Quinn, R. (2022b, March 3). *Russia-Ukraine Conflict Adds More Pressure to World Fertilizer Market*. DTN Progressive Farmer. https://www.dtnpf.com/agriculture/web/ag/news/crops/article/2022/03/03/russia-ukraine-conflict-adds-world

Randall, D. G., Krähenbühl, M., Köpping, I., Larsen, T. A., & Udert, K. M. (2016). A novel approach for stabilizing fresh urine by calcium hydroxide addition. *Water Research*, *95*, 361–369. https://doi.org/10.1016/j.watres.2016.03.007

Ray, H., Perreault, F., & Boyer, T. (2019). Urea recovery from fresh human urine by forward osmosis and membrane distillation (FO-MD). *Environmental Science: Water Research & Technology*, *5*. https://doi.org/10.1039/C9EW00720B

Ray, H., Perreault, F., & Boyer, T. H. (2020). Rejection of nitrogen species in real fresh and hydrolyzed human urine by reverse osmosis and nanofiltration. *Journal of Environmental Chemical Engineering*, *8*(4), 103993. https://doi.org/10.1016/j.jece.2020.103993

Ray, H., Perreault, F., & Boyer, T. H. (2022). Ammonia recovery and fouling mitigation of hydrolyzed human urine treated by nanofiltration and reverse osmosis. *Environmental Science: Water Research & Technology*. https://doi.org/10.1039/D1EW00601K

Ray, H., Saetta, D., & H. Boyer, T. (2018). Characterization of urea hydrolysis in fresh human urine and inhibition by chemical addition. *Environmental Science: Water Research & Technology*, *4*(1), 87–98. https://doi.org/10.1039/C7EW00271H

Ronteltap, M., Maurer, M., & Gujer, W. (2007a). Struvite precipitation thermodynamics in source-separated urine. *Water Research*, *41*(5), 977–984. https://doi.org/10.1016/j.watres.2006.11.046

Ronteltap, M., Maurer, M., & Gujer, W. (2007b). The behaviour of pharmaceuticals and heavy metals during struvite precipitation in urine. *Water Research*, *41*(9), 1859–1868. https://doi.org/10.1016/j.watres.2007.01.026

Ronteltap, M., Maurer, M., Hausherr, R., & Gujer, W. (2010). Struvite precipitation from urine – Influencing factors on particle size. *Water Research*, *44*(6), 2038–2046. https://doi.org/10.1016/j.watres.2009.12.015

Saetta, D., Padda, A., Li, X., Leyva, C., Mirchandani, P. B., Boscovic, D., & Boyer, T. H. (2019). Water and Wastewater Building CPS: Creation of Cyber-Physical Wastewater Collection System Centered on Urine Diversion. *IEEE Access*, *7*, 182477–182488. https://doi.org/10.1109/ACCESS.2019.2959992

Saetta, D., Zheng, C., Leyva, C., & Boyer, T. H. (2020). Impact of acetic acid addition on nitrogen speciation and bacterial communities during urine collection and storage. *Science of The Total Environment*, *745*, 141010. https://doi.org/10.1016/j.scitotenv.2020.141010

Save! | Design & Innovation. (n.d.). Laufen. Retrieved November 9, 2021, from https://www.laufen.com/news-stories/save-smart-sanitation-2

Shaw, K. L., Grimsley, G. R., Yakovlev, G. I., Makarov, A. A., & Pace, C. N. (2001). The effect of net charge on the solubility, activity, and stability of ribonuclease Sa. *Protein Science : A Publication of the Protein Society*, *10*(6), 1206–1215.

Sirrine, J. M., Schexnayder, S. A., Dennis, J. M., & Long, T. E. (2018). Urea as a monomer for isocyanate-free synthesis of segmented poly(dimethyl siloxane) polyureas. *Polymer*, *154*, 225–232. https://doi.org/10.1016/j.polymer.2018.09.003

Solanki, A., & Boyer, T. H. (2017). Pharmaceutical removal in synthetic human urine using biochar. *Environmental Science: Water Research & Technology*, *3*(3), 553–565. https://doi.org/10.1039/C6EW00224B

Szymczyk, A., & Fievet, P. (2005). Investigating transport properties of nanofiltration membranes by means of a steric, electric and dielectric exclusion model. *Journal of Membrane Science*, *252*(1), 77–88. https://doi.org/10.1016/j.memsci.2004.12.002

Tanford, C. (1963). The Interpretation Of Hydrogen Ion Titration Curves Of Proteins. In C. B. Anfinsen, K. Bailey, M. L. Anson, & J. T. Edsall (Eds.), *Advances in Protein Chemistry* (Vol. 17, pp. 69–165). Academic Press. https://doi.org/10.1016/S0065-3233(08)60052-2

Tarpeh, W. A., Udert, K. M., & Nelson, K. L. (2017). Comparing Ion Exchange Adsorbents for Nitrogen Recovery from Source-Separated Urine. *Environmental Science & Technology*, *51*(4), 2373–2381. https://doi.org/10.1021/acs.est.6b05816

Udert, K. M., Fux, C., Münster, M., Larsen, T. A., Siegrist, H., & Gujer, W. (2003). Nitrification and autotrophic denitrification of source-separated urine. *Water Science and Technology: A Journal of the International Association on Water Pollution Research*, *48*(1), 119–130.

Udert, K. M., Larsen, T. A., Biebow, M., & Gujer, W. (2003). Urea hydrolysis and precipitation dynamics in a urine-collecting system. *Water Research*, *37*(11), 2571–2582. https://doi.org/10.1016/S0043-1354(03)00065-4

Vasiljev, A., Simha, P., Demisse, N., Karlsson, C., Randall, D. G., & Vinnerås, B. (2022). Drying fresh human urine in magnesium-doped alkaline substrates: Capture of free ammonia, inhibition of enzymatic urea hydrolysis & minimisation of chemical urea hydrolysis. *Chemical Engineering Journal*, *428*, 131026. https://doi.org/10.1016/j.cej.2021.131026

WES-4000 | Sloan. (n.d.). Sloan. Retrieved November 9, 2021, from https://www.sloan.com/commercial-bathroom-products/urinals/sloan-vitreous-china/wes-4000

Wilsenach, J. A., Schuurbiers, C. a. H., & van Loosdrecht, M. C. M. (2007). Phosphate and potassium recovery from source separated urine through struvite precipitation. *Water Research*, *41*(2), 458–466. https://doi.org/10.1016/j.watres.2006.10.014

Wilsenach, J., & van Loosdrecht, M. (2003). Impact of separate urine collection on wastewater treatment systems. *Water Science and Technology: A Journal of the International Association on Water Pollution Research*, *48*(1), 103–110.

Wu, C., Liu, S., Wang, Z., Zhang, J., Wang, X., Lu, X., Jia, Y., Hung, W.-S., & Lee, K.-R. (2016). Nanofiltration membranes with dually charged composite layer exhibiting super-high multivalent-salt rejection. *Journal of Membrane Science*, *517*, 64–72. https://doi.org/10.1016/j.memsci.2016.05.033

Xu, K., Zhang, C., Li, J., Cheng, X., & Wang, C. (2017). Removal and recovery of N, P and K from urine via ammonia stripping and precipitations of struvite and struvite-K. *Water Science and Technology: A Journal of the International Association on Water Pollution Research*, *75*(1–2), 155–164. https://doi.org/10.2166/wst.2016.494

Zhong, R. (2021, December 6). This Chemical Is in Short Supply, and the Whole World Feels It. *The New York Times*. https://www.nytimes.com/2021/12/06/business/urea-fertilizer-food-prices.html

APPENDIX A

SUPPEMENTARY FIGURES

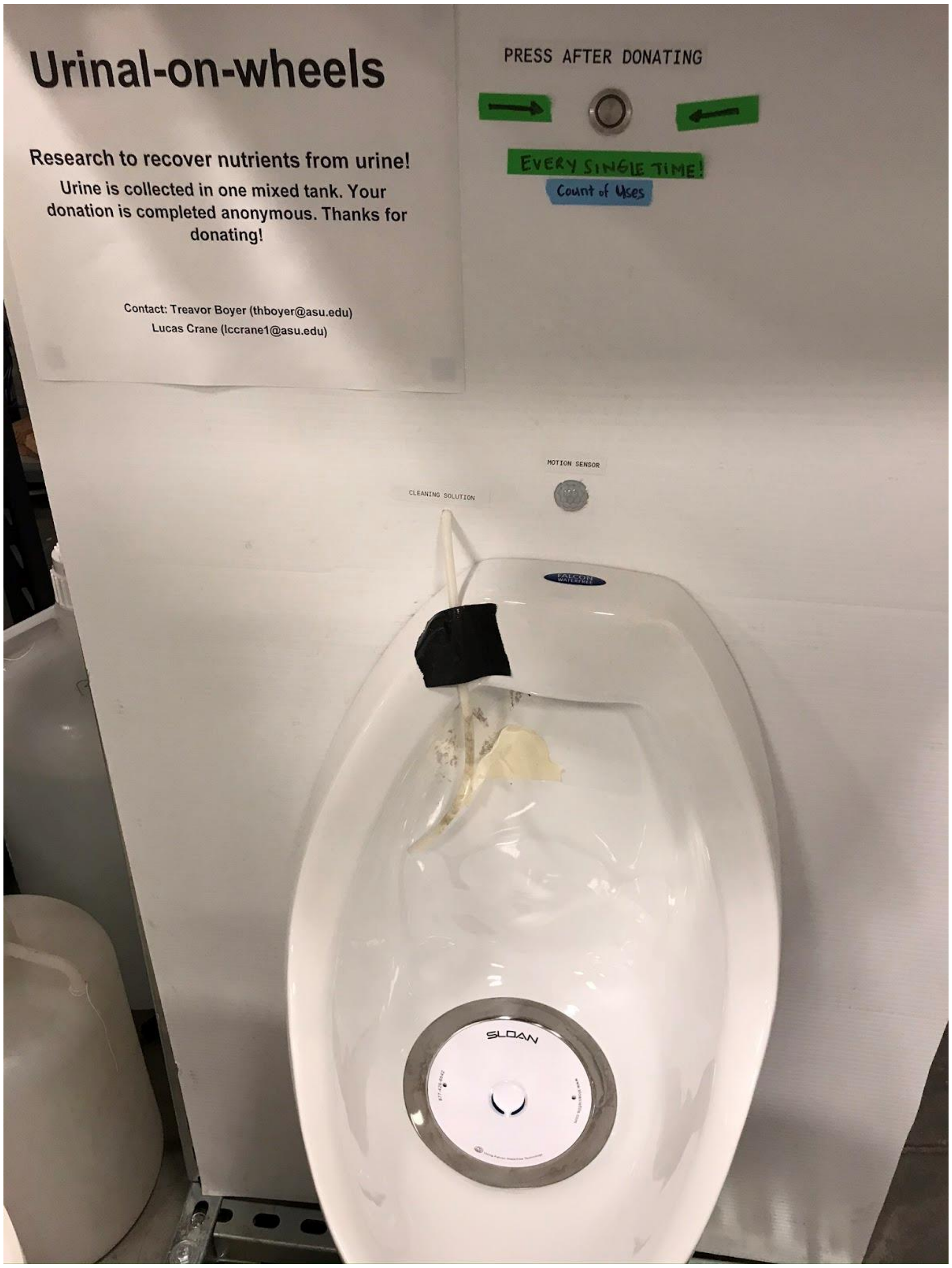

Figure S1. Portable urinal used to collect human urine. Acetic acid is pumped into the urinal based on previous algorithms optimized for maintaining a low pH. A motion sensor and a button are used to count users.

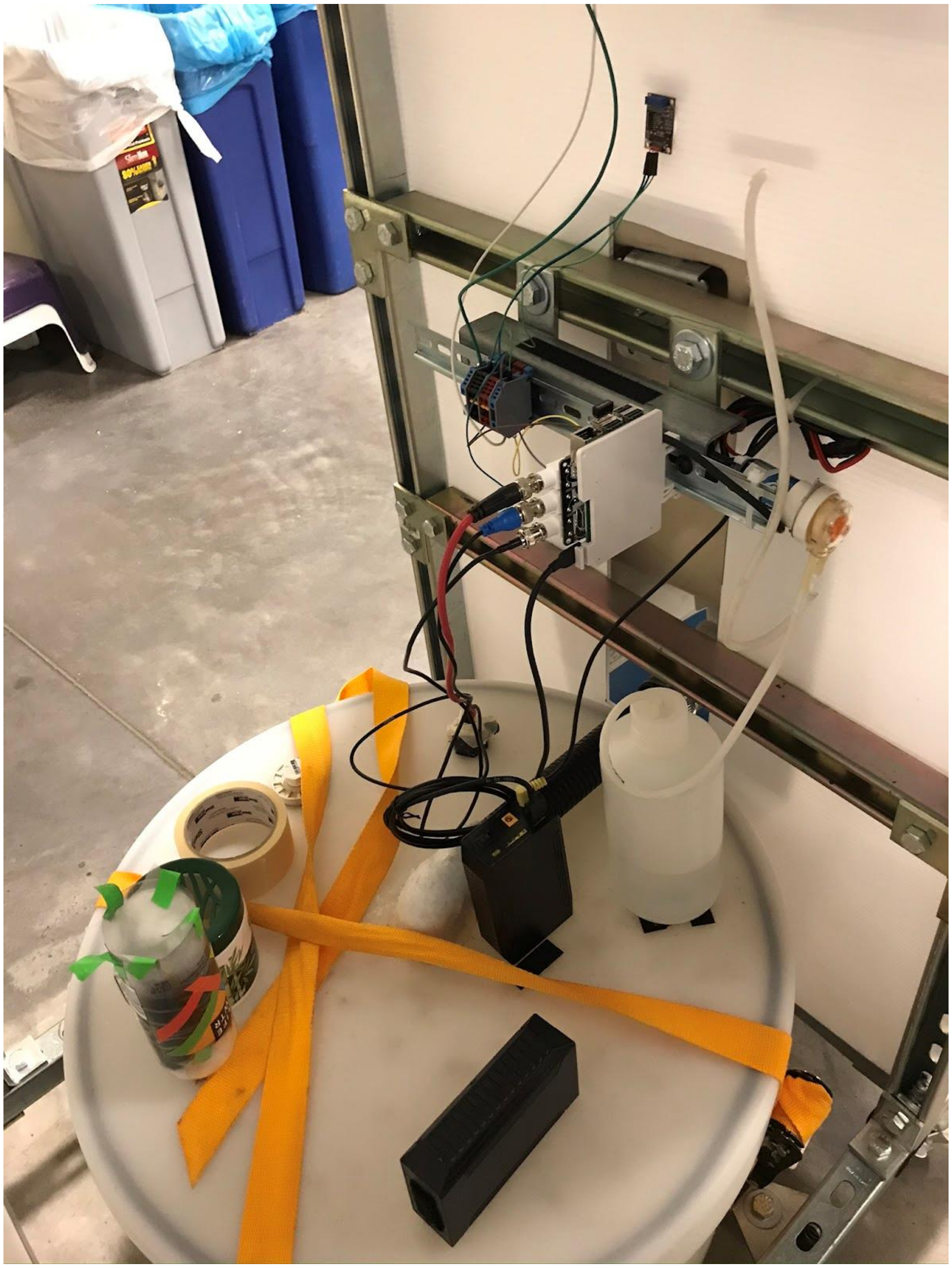

Figure S2. Inside of portable urinal. Sensors are connected to a RaspberryPi that measure pH, conductivity, and temperature of the collected urine. Acetic acid is pumped into the urinal. The tank, capable of holding 25 gallons of urine, is tightly secured down to reduce contamination of urine with microorganisms found in restrooms.

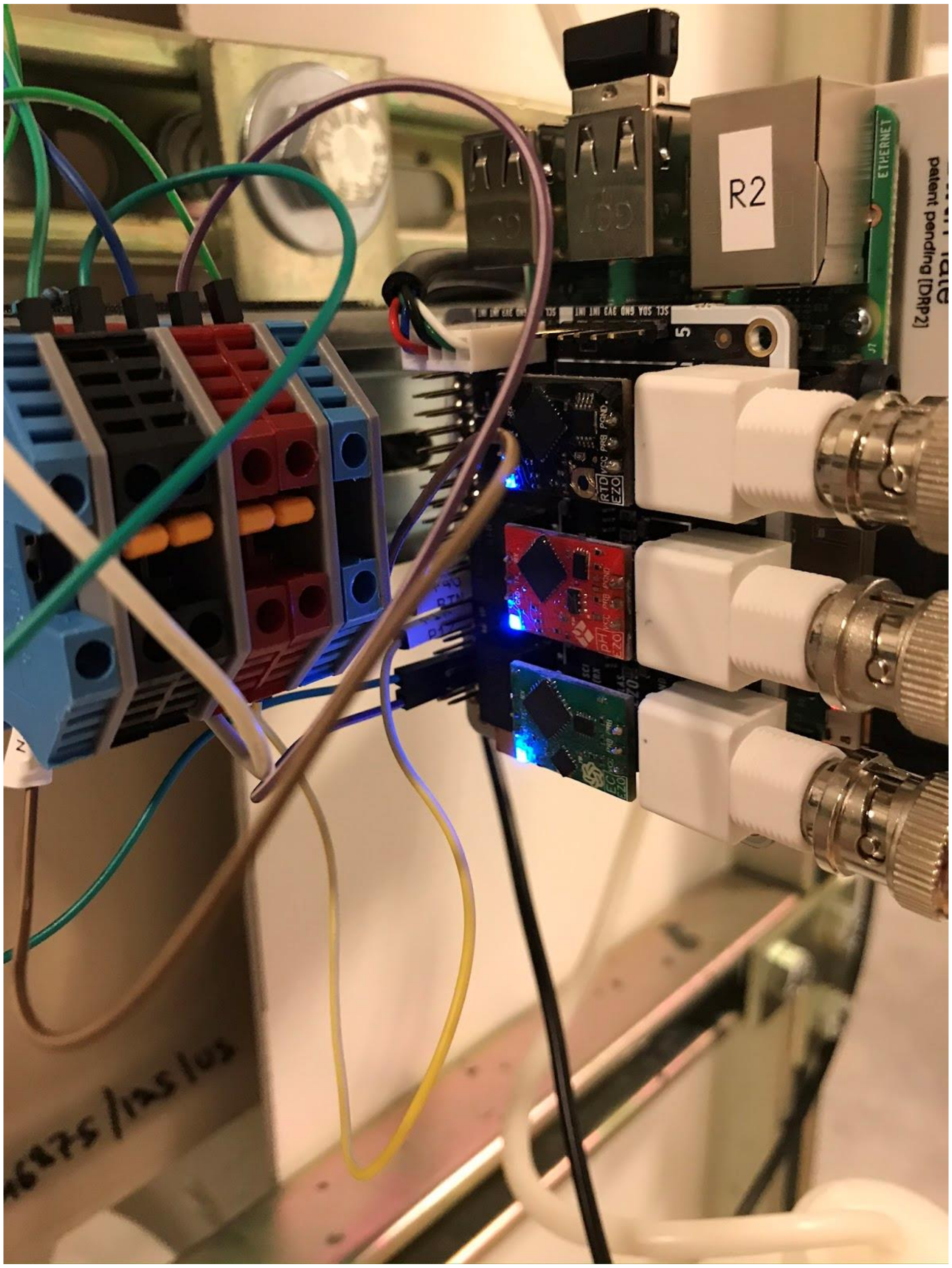

Figure S3. Close-up of RaspberryPi sensor connections. AtlasScientific sensor kits are used to measure pH, conductivity, and temperature.

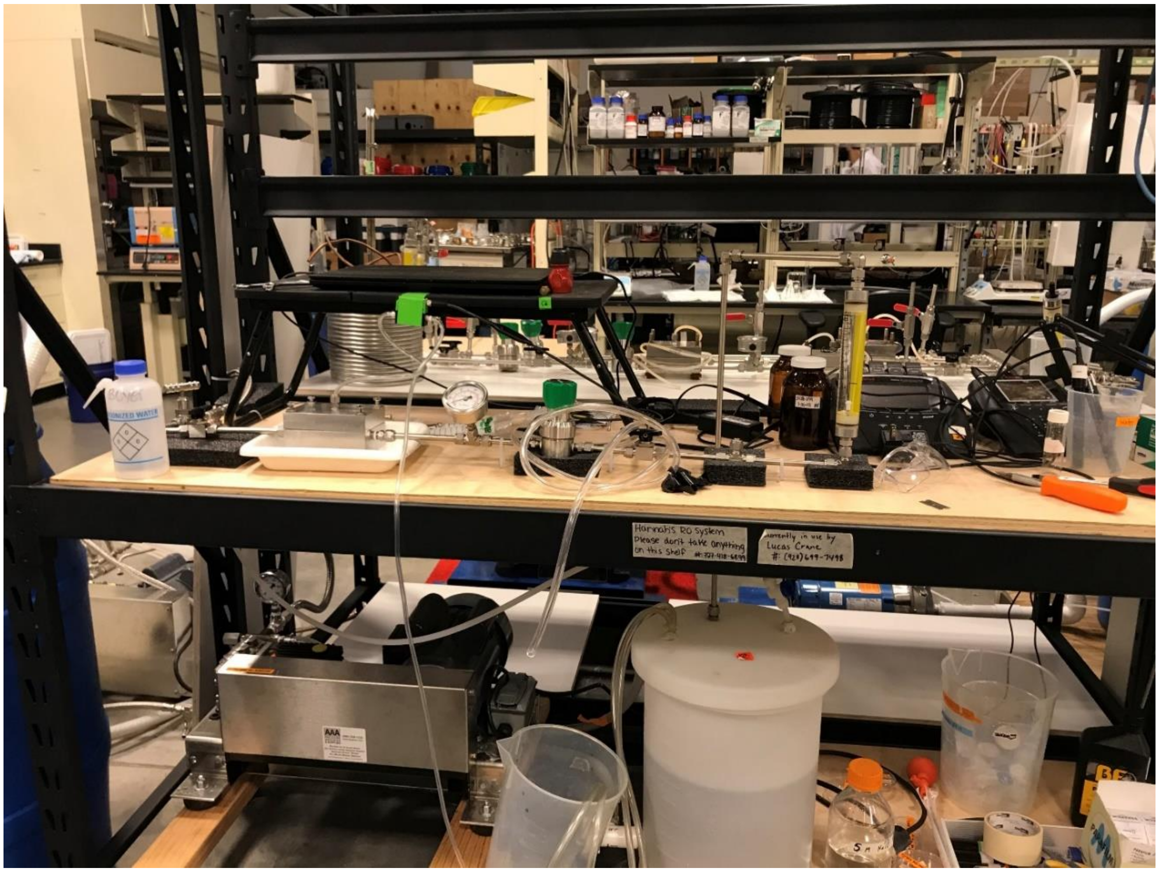

Figure S4. Overall picture of RO/NF membrane system.

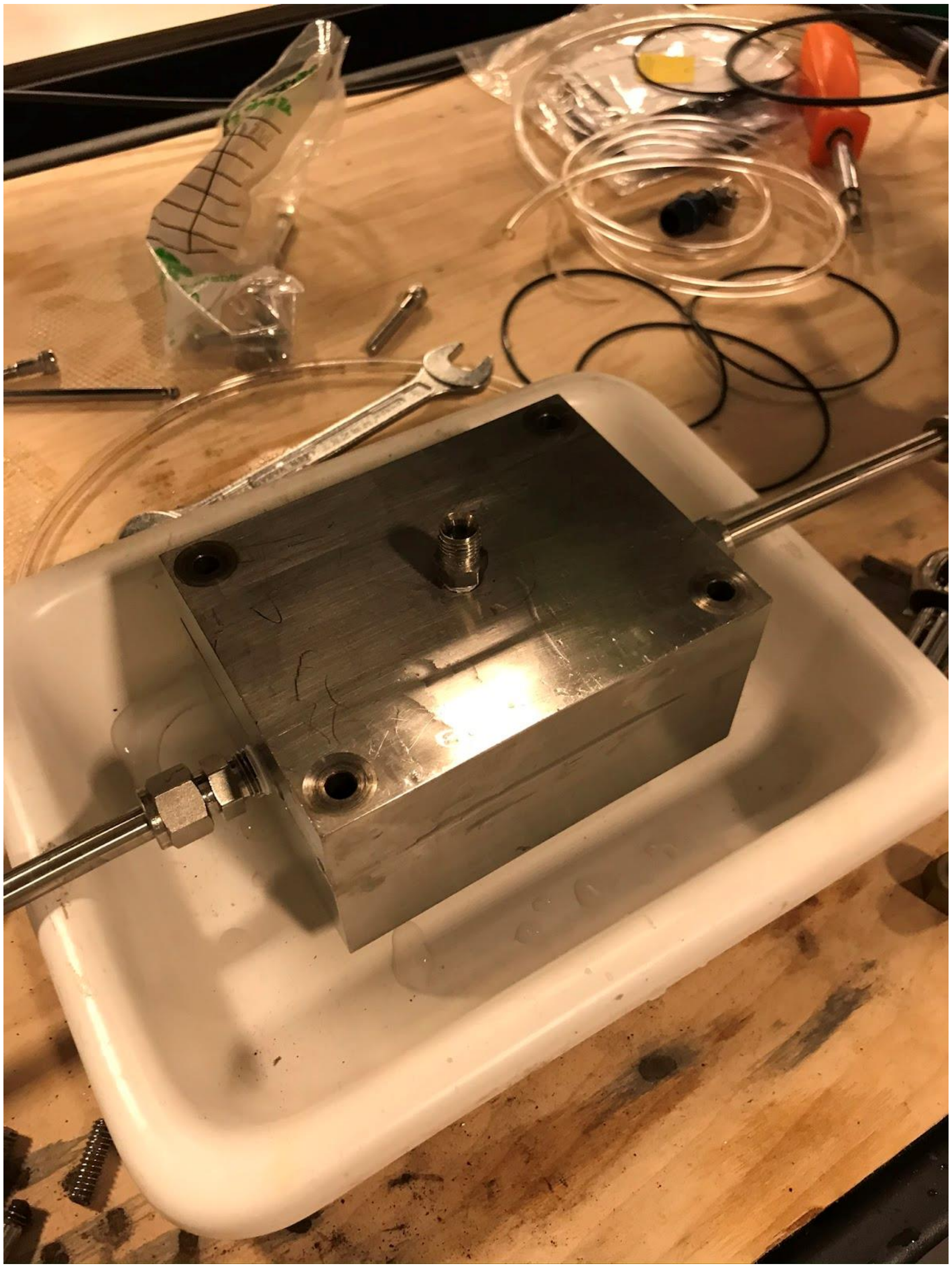

Figure S5. Membrane cell made by ASU Machine Shop; feed solution enters from the left, and retentate solution leaves on the right. Permeate solution passes through membrane and is collected via a tube on the top of the cell.

Figure S6. Flow meter (Cole-Parmer) for the retentate solution; operating conditions are at 1 LPM flow and 375 psi.

Figure S7. High-pressure pump for system. Feed solution enters from the right, travels through the pump, and exits in the top tube towards the membrane cell.

Figure S8. Microfilter system used for microfiltration of real human urine. The left cartridge is a 1-µm sediment filter, and the right cartridge is a 0.2-µm sediment filter.

Figure S9. Microfiltration of real human urine. Urine is pumped through a MasterFlex peristaltic pump at 1000 mL/min through the microfilter system at a pressure between 20–60 psi.

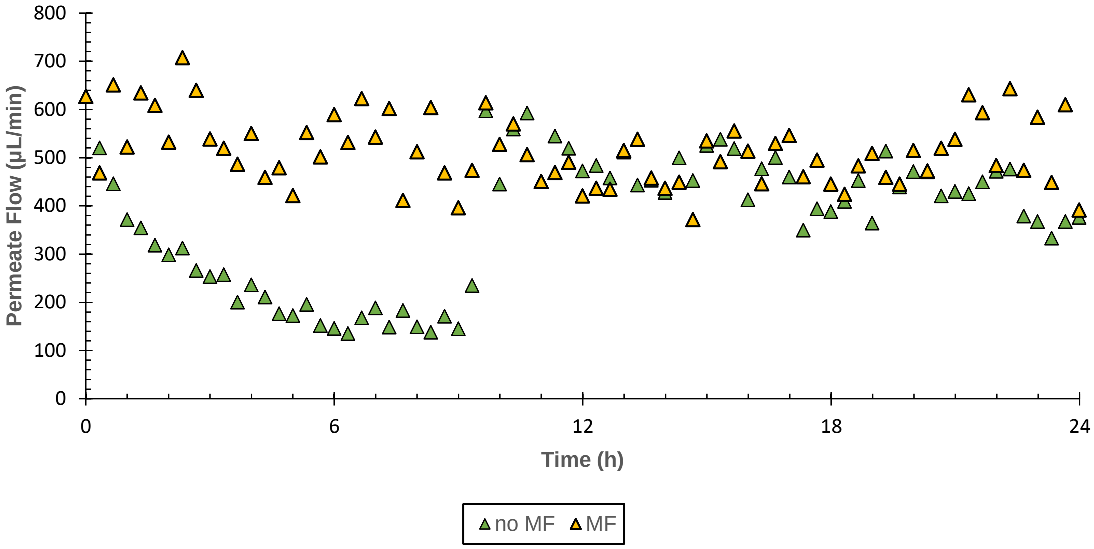

Figure S10. Duplicate results for permeate flow reduction during fouling mitigation experiments. While the duplicate experiment with no MF pretreatment experienced a significant dip in permeate flow due to feed flow reduction, the final permeate flow was still lower than the duplicate with MF pretreatment.

APPENDIX B

SUPPLEMENTARY TABLES

Table S1

Synthetic fresh urine composition, pre-dilution with existing DI water in system.

Chemical	**Concentration (g/L)**	**Concentration (M)**
Urea	15.0075	0.25
NaCl	2.5715	0.044
Na_2SO_4	2.1305	0.015
KCl	2.982	0.04
$MgCl_2 \cdot 6H_2O$	0.813	0.004
$Na_2H_2PO_4$	2.3995	0.02
$CaCl_2 \cdot 2H_2O$	0.588	0.004

Table S2

Manufacturer specifications of polyamide membranes (*Dow Filmtec Membranes | Flat Sheet Membrane Chart*, n.d.).

Membrane	**Permeate flux rate (gpd/ft^2)**	**Minimum salt rejection (%)**	**pH Range**	**Membrane Type**
BW30 RO	26	99.5	2–11	Polyamide Thin-Film Composite
NF90	21.6	97	3-10	Polyamide Thin-Film Composite
NF270	31.25	97	3-10	Polyamide Thin-Film Composite

Table S3

Composition of fixative solution for SEM analysis.

Constituent	**Concentration**
Paraformaldehyde	2%
Glutaraldehyde	2.5%
Sodium Phosphate Buffer	0.1 M